1978

Development of a quadratic finite element solution of the convective-transport equation.

David A. Dillard

Department:

DEVELOPMENT OF A QUADRATIC FINITE ELEMENT SOLUTION OF THE CONVECTIVE-TRANSPORT EQUATION

BY

DAVID A. DILLARD, 1954-

A THESIS

Presented to the Faculty of the Graduate School of the

UNIVERSITY OF MISSOURI-ROLLA

In Partial Fulfillment of the Requirements for the Degree

MASTER OF SCIENCE IN ENGINEERING MECHANICS

1978

T4400
c. 1
72 pages

Approved By

Robert L. Davis (Advisor) Ronald A. Kohser

Harold Dean Keith

PUBLICATION THESIS OPTION

This thesis has been prepared in the form of two papers for publication. Pages 1 through 36 have been prepared for publication by the American Society of Mechanical Engineers in the Journal of Heat Transfer. Pages 37 through 63 have been prepared for publication in the International Journal of Numerical Methods in Engineering. The remainder of the thesis was prepared in standard thesis format.

ABSTRACT

A quadratic finite element has been developed for the solution of the general three-dimensional convective-transport equation. Inherent instabilities in the numerical solution arise when the convective terms in the governing equation become significant. An application of upwinding techniques to the 20 degree of freedom serendipity element failed to produce acceptable results. Upwinding was applied to the 27 degree of freedom Lagrangian element with good results. Results of the latter element are given for several problems, including a model of a round to round metal forming process.

ACKNOWLEDGEMENTS

The author wishes to express his sincerest gratitude to his advisor, Professor R. L. Davis, for his guidance, assistance, encouragement, and understanding. From his suggestion of the thesis topic, through the frustrations of the development and the satisfaction of obtaining final results, to meeting deadlines at the end, he has been most helpful. A special thanks is also extended to the other committee members: Professor H. D. Keith for his valuable insights and recommendations in the areas of finite element and numerical techniques, and for reading the manuscript; and Profssor R. A. Kosher for reading the manuscript. The author is grateful to the Engineering Mechanics Department of the University of Missouri-Rolla for providing a teaching assistantship and obtaining computer funds, and to the National Science Foundation for financial support. The author is deeply grateful to his parents for their support, concern, and understanding throughout his education. Finally, a special thanks to Vicki Hudgins, Vicki Snelson, and Cheryl Abbott for their patience in typing the manuscript in various stages of the development.

TABLE OF CONTENTS

LIST OF ILLUSTRATIONS

PAPER 1

PAPER II

LIST OF TABLES

A QUADRATIC FINITE ELEMENT FOR THE THREE-DIMENSIONAL CONVECTIVE-TRANSPORT EQUATION

Prepared for

JOURNAL OF HEAT TRANSFER

AMERICAN SOCIETY OF MECHANICAL ENGINEERS

Written by

DAVID A. DILLARD AND ROBERT L. DAVIS

David A. Dillard
Graduate Student, Dept. of Engineering Mechanics
University of Missouri-Rolla
Rolla, MO

Robert L. Davis
Assistant Dean, School of Engineering
Professor, Dept. of Engineering Mechanics
University of Missouri-Rolla
Rolla, MO

ABSTRACT

A three-dimensional quadratic element has been developed for the analysis of thermal phenomena in general metal forming operations. In order to model production speeds, upwinding schemes were incorporated to eliminate the inherent solution instabilities that occur at high velocities. Serious difficulties were encountered in applying upwind schemes to a serendipity element, forcing the use of a Lagrangian element. Typical results for the temperature distribution in a round to round extrusion process are shown, based on a velocity field described by Avitzur.

INTRODUCTION

Quasi-continuous forming operations--drawing and extruding--are commercially important processes for mass production of metal goods. High speed production, reduced machining requirements, low scrap losses, improved mechanical properties, one piece construction, and resultant energy savings promise continuing development for these production techniques. Methods of analysis of the process are required for improving production rate, quality of the product, and longevity of the equipment. An understanding of the flow field, the behavior of the material, induced stress state, and temperature distribution is helpful for selecting and optimizing the process variables such as extrusion rate, reduction in area, die angle, initial billet temperature, die cooling, and lubrication conditions. Traditionally, analytic plasticity solution techniques have been available for only very simple geometries and then only if some very simplifying assumptions are made about the behavior of the material being deformed. Methods of analysis for complex geometries and detailed material behavior have been quite elusive, although in very recent years, progress has been made in this area by applying numerical schemes to the problem [1-6].[1]

Several mathematical formulations have been used in conjunction with finite element techniques to analyze forming processes. Perhaps one of the most promising of these theoretical methods has been the Upper Bound limit analysis. A three dimensional finite element computer program utilizing this approach is currently being developed at the

[1] Numbers in brackets designate References at end of paper.

University of Missouri-Rolla [6]. The program, entitled FEDA (Finite Element Deformation Analysis) is currently in the refinement stage to make it applicable to industrial process analysis. Incorporating a rapidly converging iterative scheme, the program finds kinematically admissible strain rate fields which successively tend to minimize the power expression prescribed by the Upper Bound Theorem.

The purpose of this paper is to develop a refined element for thermal analysis to be incorporated into FEDA. Certainly, temperature has a very marked effect on material properties. Results of Davidson and Davis [7] indicate a reduction in effective yield strength of perhaps 50% for 6061-T651 aluminum within the length of the die, due simply to a temperature build up of 300^{o}C for a typical extrusion. Properties of lubricants are also very temperature dependent - most lubricants having a specific temperature range in which they will perform satisfactorily. The life of costly dies is also related to temperature via the friction induced wear and the associated die strength. Because of these temperature effects, it is necessary to provide accurate means for the thermal analysis of the extrusion process, including the die.

The proposed solution is a finite element which permits transient, three-dimensional, thermal analysis of general continuous forming operations. It permits various complex geometries of the extrusion, general convective boundary conditions on all non-adjoining surfaces, anisotropic thermal conductivities; heat generation in regions of deformation and at frictional surfaces; and accounts for extrusion rate and losses into surrounding dies, etc. Finally, the formulation is compatible with FEDA, where it will soon be incorporated.

THE VARIATIONAL STATEMENT

The thermal behavior obeys the convective transport equation:

$$\text{DE:} \quad \rho c\left(\frac{\partial T}{\partial t} + u_i T_{,i}\right) = \left(k_{ij} T_{,j}\right)_{,i} + Q \qquad \text{on } V \qquad (1)$$

$$\text{BC:} \quad a_1 T + a_2 k_{ij} T_{,j} \nu_i = a_3 \qquad \text{on } S \qquad (2)$$

$$\text{IC:} \quad T = T_o(x, y, z) \text{ at } t = 0 \qquad \text{on } V \qquad (3)$$

where ρ is the density; c, the specific heat; $\partial T/\partial t$, the time derivative of temperature; u_i, the velocity components; T, the temperature; $k_{ij} (= k_{ji})$, the thermal conductivities; Q the heat source; a_1, a_2, and a_3, are known functions describing the boundary conditions; V, is the body being considered; ν_i, the direction cosines of a vector normal to dS; and S is the surface of the body.

For convenience, let

$$\Omega = a_1/a_2 \qquad (4)$$

$$\Psi = a_3/a_2 \qquad (5)$$

Provisions for the special case of $a_2 = 0$, will be made later. No generality is lost by writing it in this form for now, however.

The weighted residual expression [8] of the problem may be written as

$$\int_V \left[\rho c\left(\frac{\partial T}{\partial t} + u_i T_{,i}\right) - \left(k_{ij} T_{,j}\right)_{,i} - Q\right] W \, dV \qquad (6)$$

$$+ \int_S \left[k_{ij} T_{,j} \nu_i + (\Omega T - \Psi)\right] W \, dS = 0,$$

where W is some appropriately chosen weighting function. Application of the divergence theorem[1] allows one to write

$$\int_V \{[\rho c(\frac{\partial T}{\partial t} + u_i T_{,i}) - Q] W + k_{ij} T_{,j} W_{,i}\} dV + \int_S (\Omega T - \Psi) W dS = 0 \quad (7)$$

[1] See Appendix A.

THE FINITE ELEMENT TECHNIQUE

To apply the finite element technique to the variational statement, a discrete number of nodal points are selected throughout and on the surface of the body being analyzed. The value of some parameter, u, at any point (x, y, z) within the body will be approximated as the sum of the products of the value of u at the nodal points and some interpolation functions, ϕ_i, for all nodal points

$$u = \phi_1 u_1 + \phi_2 u_2 + \ldots + \phi_n u_n = \sum_{i=1}^{n} \phi_i u_i = \{\phi\}^T \{u^n\} \tag{8}$$

where ϕ_i is the interpolation function associated with node i evaluated at (x, y, z); and $\{u^n\}$ is the vector of nodal values of the parameter u. While the selection of the interpolation functions is somewhat arbitrary, they must be chosen to satisfy admissibility and completeness.

Application of this method of approximations to the unknowns of our problem yields

$$T = \{\phi\}^T \{T^n\} \tag{9}$$

$$T_{,i} = \{\phi_{,i}\}^T \{T^n\} \tag{10}$$

$$\frac{\partial T}{\partial t} = \{\phi\}^T \{\frac{\partial T^n}{\partial t}\} \tag{11}$$

The weighting functions are commonly taken to be the same as the interpolation functions, resulting in a weight at a point of

$$W = \{\phi\}^T \{\partial T^n\} \tag{12}$$

where $\{\partial T^n\}$ is the vector of arbitrary virtual increments of temperature at each node. These Galerkin weighting functions are used extensively

in finite element programs. Instabilities arise, however, when these weighting functions are used for elliptic partial differential equations with significant first derivative terms. Thus for generality, the weight at a point is expressed as

$$W = \{\chi\}^T \{\delta T^n\} = \{\delta T^n\}^T \{\chi\} \tag{13}$$

$$W_{,i} = \{\chi_{,i}\}^T \{\delta T^n\} = \{\delta T^n\}^T \{\chi_{,i}\} \tag{14}$$

where $\{\chi\}$ may be taken the same as the interpolation functions $\{\phi\}$ for Galerkin weights, or may be taken as some other appropriate functions.

Combining these approximations for the unknowns into the weighted residual expression, Eq. (7), yields

$$\{\delta T\}^T \Bigg[\int_V [\rho c(\{\chi\} \{\phi\}^T \{\frac{\partial T^n}{\partial t}\} + u_i \{\chi\} \{\phi_{,i}\}^T \{T^n\}) - Q \{\chi\} + k_{ij} \{\chi_{,i}\} \{\phi_{,j}\}^T \{T^n\}] \, dV + \int_S [\Omega \{\chi\} \{\phi\}^T \{T^n\} - \Psi \{\chi\}] \, dS \Bigg] = 0 \tag{15}$$

Letting Π_i represent the residual statement for node i allows one to write

$$\{\delta T^n\}^T \{\Pi\} = 0 \tag{16}$$

$$\delta T_1 \Pi_1 + \delta T_2 \Pi_2 + \ldots + \delta T_n \Pi_n = 0 \tag{17}$$

Because the δT_i are arbitrary, this equation will be satisfied only if

$$\Pi_1 = \Pi_2 = \ldots = \Pi_n = 0 \tag{18}$$

$$\{\Pi\} = \{0\} \tag{19}$$

This may be expressed as the classical system of equations:

$$\tilde{C}\ \{\frac{\partial T^n}{\partial t}\} + \tilde{H}\ \{T^n\} = \{F\} \tag{20}$$

where

$$\tilde{C} = \int_V \rho c\ \{\chi\}\ \{\phi\}^T\ dV \tag{21}$$

$$\tilde{H} = \int_V \rho c u_i\ \{\chi\}\ \{\phi_{,i}\}^T\ dV + \int_V k_{ij}\ \{\chi_{,i}\}\ \{\phi_{,j}\}^T\ dV + \int_S \Omega\ \{\chi\}\ \{\phi\}^T\ dS \tag{22}$$

$$\{F\} = \int_V Q\ \{\chi\}\ dV + \int_S \Psi\{\chi\}\ dS \tag{23}$$

The transient analysis is forthcoming; for the purposes of this paper, however, we will only consider the steady state problem. Since $\{\partial T^n/\partial t\} = \{0\}$, the system of equations is simplified to

$$\tilde{H}\ \{T^n\} = \{F\} \tag{24}$$

Note that the system of equations is symmetric only if $\{\phi\} = \{\chi\}$ and if $\rho c u_i = 0$. Thus, in general, decomposition of a non-symmetric matrix must be performed.

The essential boundary condition requirement will be satisfied if there is some integrable surface area over which Ω is non-zero. The specified temperature boundary condition is simply a special case of Eq. (2) in which $a_2 = 0$. As $a_2 \to 0$, $\Omega(= a_1/a_2)$ and $\Psi(=a_3/a_2)$ will dominate the residual statement, Eq. (7). In the limit, when $a_2 = 0$, the residual expression becomes

$$\Omega T - \Psi = 0 \tag{25}$$

Alternatively, essential boundary conditions may be imposed at any nodal point i by specifying a temperature T_o at that node. Because T_i is fixed, $\delta T_i = 0$ and the weighted residual statement is replaced by

$$[0 \quad 0 \ldots 1 \ldots 0] \{T^n\} = T_o \tag{26}$$

$$T_i = T_o \tag{27}$$

Finally, discretization of the body into elements connected at some of the node points provides a convenient framework for establishing the interpolation functions and accounting for variations in material properties and boundary conditions. A hexahedron element is used for the thermal analysis to be compatible with FEDA.

To facilitate the integration throughout the volume or over the surfaces of the elements, a transformation of axes is used to map the general hexahedron into a local coordinate system (ξ , η, ζ) where the element is a simple cube [9] bounded by $\xi = \pm 1$, $\eta = \pm 1$, $\zeta = \pm 1$. Derivatives with respect to the global coordinates are given as:

$$\begin{Bmatrix} \frac{\partial}{\partial x} \\ \frac{\partial}{\partial y} \\ \frac{\partial}{\partial z} \end{Bmatrix} = \tilde{J}^{-1} \begin{Bmatrix} \frac{\partial}{\partial \xi} \\ \frac{\partial}{\partial \eta} \\ \frac{\partial}{\partial \zeta} \end{Bmatrix} \tag{28}$$

where $\tilde{J}$ is the Jacobian matrix given by

$$\tilde{J} = \begin{bmatrix} \frac{\partial x}{\partial \xi} & \frac{\partial y}{\partial \xi} & \frac{\partial z}{\partial \xi} \\ \frac{\partial x}{\partial \eta} & \frac{\partial y}{\partial \eta} & \frac{\partial z}{\partial \eta} \\ \frac{\partial x}{\partial \zeta} & \frac{\partial y}{\partial \zeta} & \frac{\partial z}{\partial \zeta} \end{bmatrix} \tag{29}$$

For isoparametric element formulation, the interpolation functions defining the geometry and unknown parameters are the same. For non-isoparametric element formulation, the two sets of interpolation functions are different. For a set of $\{\theta\}$ evaluated at point (ξ, η, ζ), the global coordinates of that point are given by

$$\begin{Bmatrix} x \\ y \\ z \end{Bmatrix} = \begin{bmatrix} x_1 & x_2 & \cdots & x_n \\ y_1 & y_2 & \cdots & y_n \\ z_1 & z_2 & \cdots & z_n \end{bmatrix} \begin{Bmatrix} \theta_1 \\ \theta_2 \\ \vdots \\ \theta_n \end{Bmatrix} \tag{30}$$

where (x_i, y_i, z_i) are the coordinates of node i, $\{\theta^n\}$ is the vector of geometry shape functions which may or may not be the same as the interpolation functions $\{\phi^n\}$, and n is the number of geometry points defined per element.

A typical derivative term is

$$\frac{\partial x}{\partial \xi} = \{x^n\}^T \left\{\frac{\partial \theta^n}{\partial \xi}\right\} \tag{31}$$

These derivative terms are then combined to form the Jacobian matrix, $\tilde{J}$. Using Gaussian quadrature, numerical integration is performed over the cube:

$$\iiint_V F(x, y, z)\, dxdydz = \int_{-1}^{1}\int_{-1}^{1}\int_{-1}^{1} F(x, y, z)\ |\tilde{J}|\ d\xi d\eta d\zeta$$

$$= \sum_{i=1}^{n_1} \sum_{j=1}^{n_2} \sum_{k=1}^{n_3} H_i^{n_1} H_j^{n_2} H_k^{n_3} F'(\lambda_i^{n_1}, \lambda_j^{n_2}, \lambda_k^{n_3})\ |\tilde{J}| \tag{32}$$

and for a typical face, say $\zeta = 1$:

$$\iint_S F(x, y, z)\, dS = \int_{-1}^{1}\int_{-1}^{1} \Gamma\, F(x, y, z)\, d\xi d\eta \tag{33}$$

$$= \sum_{i=1}^{n_1} \sum_{j=1}^{n_2} H_i^{n_1} H_j^{n_2} F'(\lambda_i^{n_1}, \lambda_j^{n_2}, 1)\, \Gamma(\lambda_i^{n_1}, \lambda_j^{n_2})$$

where $F'(\xi, \eta, \zeta) = F(x, y, z)$; the orders of numerical integration along ξ, η, and ζ are n_1, n_2, and n_3, respectively; $H_m^{n_\ell}$ and $\lambda_m^{n_\ell}$ are the weight and abscissa for the m^{th} quadrature point in n_ℓ order integration; $|\tilde{J}|$ is the Jacobian (det $\tilde{J}$) evaluated at $(\lambda_i^{n_1}, \lambda_j^{n_2}, \lambda_k^{n_3})$; and Γ is evaluated at $(\lambda_i^{n_1}, \lambda_j^{n_2})$ as:

$$\Gamma(\xi, \eta) = \sqrt{\left|\begin{matrix} \frac{\partial x}{\partial \xi} & \frac{\partial y}{\partial \xi} \\ \frac{\partial x}{\partial \eta} & \frac{\partial y}{\partial \eta} \end{matrix}\right|^2 + \left|\begin{matrix} \frac{\partial x}{\partial \xi} & \frac{\partial z}{\partial \xi} \\ \frac{\partial x}{\partial \eta} & \frac{\partial z}{\partial \eta} \end{matrix}\right|^2 + \left|\begin{matrix} \frac{\partial y}{\partial \xi} & \frac{\partial z}{\partial \xi} \\ \frac{\partial y}{\partial \eta} & \frac{\partial z}{\partial \eta} \end{matrix}\right|^2} \tag{34}$$

THE SERENDIPITY ELEMENT

To be compatible with the 20 node hexahedron element used in FEDA, the element shown in Fig. 1 was chosen for the thermal analysis also. The 32 degree of freedom, subparametric, cubic interpolation functions used to approximate each component of velocity in the flow analysis were deemed excessive for the temperature variation. Quadratic, isoparametric interpolation functions were chosen as adequate to accurately describe the thermal behavior. [10]

Define the following one dimensional interpolation functions:

$$N_1(\xi) = \frac{1}{2}\,\xi(\xi - 1) \tag{35}$$

$$N_2(\xi) = 1 - \xi^2 \tag{36}$$

$$N_3(\xi) = \frac{1}{2}\,\xi(\xi + 1) \tag{37}$$

$$L_1(\xi) = \frac{1}{2}\,(1 - \xi) \tag{38}$$

$$L_3(\xi) = \frac{1}{2}\,(1 + \xi) \tag{39}$$

The serendipity interpolation functions for a 20 node hexahedron are given as

$$\phi = N_i(\xi)L_j(\eta)L_k(\zeta) + L_i(\xi)N_j(\eta)L_k(\zeta) \tag{40}$$

$$+ L_i(\xi)L_j(\eta)N_k(\zeta) - 2L_i(\xi)L_j(\eta)L_k(\zeta)$$

for a corner node and for mid-edge nodes as:

$$\phi = N_2(\xi)L_j(\eta)L_k(\zeta) \quad \text{for edges parallel to the } \xi \text{ axis,} \tag{41}$$

$$\phi = L_i(\xi)N_2(\eta)L_k(\zeta) \quad \text{for edges parallel to the } \eta \text{ axis,} \tag{42}$$

$$\phi = L_i(\xi)L_j(\eta)N_2(\zeta) \quad \text{for edges parallel to the } \zeta \text{ axis,} \tag{43}$$

where i, j, k refer to the location of the node with respect to the ξ, η, and ζ axes, respectively. For example:

$$i = \begin{cases} 1 & \text{for nodes at } \xi = -1 \\ 2 & \text{for nodes at } \xi = 0 \\ 3 & \text{for nodes at } \xi = 1 \end{cases} \tag{44}$$

Utilizing these serendipity interpolation functions for approximating both geometry and temperature variation, and taking the weighting functions $\{\chi\}$ to be the same as the interpolation functions $\{\phi\}$, we obtain the formulation for the three-dimensional serendipity element.

The element behaves well, yielding essentially exact solutions to one-dimensional rod problems with various boundary conditions and internal heat generation. The solution becomes unstable, however, when the convective term in the governing partial differential equation becomes significant.

THE UPWIND TECHNIQUE

The literature indicates that solution instabilities can be found in the older finite difference techniques, as well as finite element methods [11-14]. Instabilities with finite difference methods were avoided by the use of an upwind, rather than central difference stencil, in which the derivatives of temperature are based on the upstream nodal temperatures.

Heinrich and Zienkiewicz have applied a similar technique to one dimensional quadratic finite element formulations by using non-symmetric weighting functions given by

$$W_i = W_i(\xi, \alpha) = N_i(\xi) - \alpha F(\xi) \quad \text{for nodes 1 and 3} \tag{45}$$

$$W_2 = W_2(\xi, \beta) = N_2(\xi) + 4\beta F(\xi) \quad \text{for node 2} \tag{46}$$

where

$$F(\xi) = \frac{5}{8}\,\xi(\xi - 1)(\xi + 1) \tag{47}$$

$F(\xi)$ forms the non-symmetric contribution to the weighting functions and is shown in Fig. 2. The local, or element, Peclet number is defined as

$$\gamma = \left| \frac{uh}{\kappa} \right| \tag{48}$$

where u is the velocity; h, the element mesh size; and $\kappa = \frac{k}{\rho c}$. Instabilities in the solution are predicted when this local Peclet number exceeds a value of 4.0 for the element. Heinrich goes on to show that for the case of no heat generation, constant velocity, regular mesh size of h, steady state, and specified temperature boundary conditions, there are optimal values of α and β which, when

used in the weighting functions, will reproduce the exact solutions at each node. These optimal parameter values are:

$$\beta_0 = \coth\left(\frac{\gamma}{4}\right) - \frac{4}{\gamma} \tag{49}$$

$$\alpha_0 = 2\tanh\left(\frac{\gamma}{2}\right)\left(1 + \frac{3\beta_0}{\gamma} + \frac{12}{\gamma^2}\right) - \frac{12}{\gamma} - \beta_0 \tag{50}$$

The sign of α_0 and β_0 is taken to be the same as that of the velocity, u. Heinrich then proposes that these concepts may be applied to two-dimensional Lagrangian (9 node) and serendipity (8 node) elements. While the application to the Lagrangian elements is very straightforward, the extension to the serendipity elements is not obvious. In fact, no satisfactory method was found to map the one-dimensional weights throughout the three-dimensional serendipity element. The problem lies in the coupling between ξ, η, and ζ in the serendipity interpolation functions which do not easily lend themselves to simple blending techniques as do the Lagrangian interpolation functions. Therefore, the serendipity element was abandoned in favor of the Lagrangian element.

THE LAGRANGIAN ELEMENT

The quadratic, three-dimensional, Lagrangian element [10], shown in Fig. 3, contains 27 nodes--an additional 6 mid-face nodes and a mid-element node more than the serendipity element. To avoid the need for inputting the coordinates and velocities of these extra nodes, the element used is subparametric--more nodes describing the temperature variation than describing the element geometry. The Jacobian, Jacobian matrix, coordinate transformations, and velocity variation are still given by the serendipity shape functions of Eq. (40-43). The temperature variation, however, is now given by the Lagrangian interpolation functions,

$$\phi = N_i(\xi)N_j(\eta)N_k(\zeta) \quad \text{for all 27 nodes} \tag{51}$$

The extension of the modified weights to this three-dimensional element is simply

$$\chi = W_i(\xi)W_j(\eta)W_k(\zeta) \tag{52}$$

A set of upwind parameters (α_o and β_o) is associated with each edge of the element, lines through the mid-face nodes, and through the mid-element node for a total of 27 sets of parameters. Along each of these lines, α_o and β_o are calculated according to Eq. (49, 50). Defining nodes 1, 2, and 3 as in Eq. (44), the velocity along a line thru these nodes is

$$u = \frac{1}{6}(\vec{u}_1 + 4\vec{u}_2 + \vec{u}_3) \cdot \hat{t} \tag{53}$$

where $\hat{t}$ is a unit vector directed from node 1 to node 3. The mesh size is taken as the distance between nodes 1 and 3. By simple transformation of a second order tensor, the conductivity along $\hat{t}$ for a non-isotropic material is given as

$$k = l^2 k_{11} + m^2 k_{22} + n^2 k_{33} + 2lm\, k_{12} + 2ln\, k_{13} + 2mn\, k_{23} \quad (54)$$

where l, m and n are direction cosines of $\hat{t}$ with respect to the global coordinate system.

Knowing these upwind parameters for a given element, we can calculate the value of modified weighting function at each point within the element. Allowing the amount of upwinding to be optimized for each element, even when $\gamma < 4$, produces very good results for the element.

RESULTS

The accuracy of the elemetn formulation has been evaluated for a variety of configurations. The results obtained agree quite well with closed form solutions available. Results for several problems are given below; the interested reader is referred to reference (15) for other aspects in the assessment of the element's capabilities.

Fig. 4 illustrates a solution typical for the temperature distribution of a moving medium with one-dimensional geometry. The results are for the downstream end of a 10-element model of a material moving with a constant velocity to the right. The inlet temperature was specified as 0.0, the exit temperature as 1.0, and the other exposed surfaces were insulated. The finite element solution results agree to 8 digits with the analytic solution. The instabilities induced without upwinding are also indicated.

The thermal analysis of a metal forming process may be conducted independently of FEDA if a velocity field is assumed a priori and if certain assumptions are made about the material characteristics. Utilizing the velocity field for flow through a conical die as described by Avitzur [16], a simple round to round aluminum extrusion was modeled as shown in Figs. 5 and 6. The yield strength, σ_o, of the aluminum was assumed to be a constant, 345 MPa (50 ksi). Because of symmetry, there is no flux across radial planes, and a quarter section could be used for the modesl. Constant friction of $(m\sigma_o/\sqrt{3})$ was assumed at the die-product interface, where m is the friction parameter. Heat generation was modeled according to the velocity field. The mechanical to thermal energy conversion was taken as 90%.

The film coefficients for simulated convective boundary conditions modeling exposure of the process to ambient air at 21.1°C (70°F) were specified as follows: billet and product end faces, 383.3 $W/m^2 \cdot K$; cylindrical surfaces of billet and product, 8.96 $W/m^2 \cdot K$; end faces of die, 8.96 $W/m^2 \cdot K$; cylindrical surface of die, 7.20 $W/m^2 \cdot K$. Due to the upwinding, the temperatures at the upstream end must be specified for higher velocities to ensure that the entrance temperature will match the ambient temperature. This boundary condition was used for velocities of .2 m/sec and greater for the model discussed. For the model of a 30° die half angle and an extrusion ratio of 2.0, the element Peclet number for elements within the deformation zone exceeds the critical value of 4.0 for velocities greater than .095 m/sec (18.6 ft/min). Results of the finite element model are compared with inlet to exit temperature increases predicted by analytic integration of the power required for the assumed velocity field over the deformation zone (modeled by elements 4 and 5), the spherical surfaces of velocity discontinuity (elements 3 and 6), and the frictional surfaces (elements 16-21); and corresponds to the billet undergoing an adiabatic process.

The results for an exit velocity of 1 m/sec (200 ft/min) and several die angles, extrusion ratios, and friction parameters are shown in Fig. 7 and 8. At velocities this high, the convective boundary conditions specified on all exposed surfaces of the die and product transmit an insignificant amount of power in comparison with the power of deformation, and the process is essentially adiabatic. The comparison of numerical and analytic results is particularly encouraging for the small die angles and no friction. The errors shown are quite

regular and are believed to be due to errors in modeling rather than in element performance. Fig. 9 shows the effect of velocity on the temperature increase through the length of the die. At higher velocities, the high gradients induced primarily by the flux from the friction elements creates a larger error in the results. As with other finite element approaches, one must provide finer grids in regions of high gradients to obtain reliable results. Nonetheless, the authors are encouraged by the accuracy of the coarse mesh used to model the problem.

A pre-processing package was written to generate the nodal point data for the various geometries considered. A post-processing package plots isothermals for the finite element results. A typical isothermal plot is shown in Fig. 10.

CONCLUDING REMARKS

A finite element program has been developed using a 27-degree of freedom, quadratic, Lagrangian element for the solution of the three-dimensional convective-transport equation. Upwind schemes were successfully applied to this Lagrangian element to suppress solution instabilities arising with the use of standard Galerkin weighting functions. The authors have found no acceptable means to apply similar upwind schemes to the three-dimensional, quadratic, serendipity element originally used in the investigation.

The Lagrangian element has been used to produce very good results for a variety of geometries and boundary conditions. A crude mesh used to model an extrusion process produced a rise in temperature which compared quite well with an analytic solution based on a velocity field described by Avitzur.

The thermal analysis program was developed to be used with FEDA in the analysis of general metal forming processes. The program, however, may also be used independently to solve a variety of problems of engineering interest. Possible applications include; temperature distributions around moving heat sources such as arc welding, cutting torches, or machining operations; grinding and polishing operations on objects such as glass lenses which are very sensitive to temperature buildups; and thermal behavior of laminar flow past heat sources.

APPENDIX A

APPLICATION OF DIVERGENCE THEOREM TO VARIATIONAL STATEMENT

From vector calculus, we have the divergence theorem:

$$\int_V (\nabla \cdot \bar{g}) dV = \int_S \bar{g} \cdot \bar{\nu} \; dS \tag{55}$$

where $\bar{\nu}$ is unit normal to the surface. Let $\bar{g} = \phi \bar{f}$ (56)

$$\int_V (\nabla \cdot \phi \bar{f}) dV = \int_S \phi \bar{f} \cdot \bar{\nu} \, dS \tag{57}$$

$$\int_V \nabla\phi \cdot \bar{f} + \phi(\nabla \cdot \bar{f}) dV = \int_S \phi \bar{f} \cdot \bar{\nu} \, dS \tag{58}$$

$$\int_V \phi(\nabla \cdot \bar{f}) dV = \int_S \phi \bar{f} \cdot \bar{\nu} \, dS - \int_V \nabla\phi \cdot \bar{f} \, dV \tag{59}$$

Now let:

$$\phi = W \tag{60}$$

$$\bar{f} = -f_x \hat{i} - f_y \hat{j} - f_z \hat{k} \tag{61}$$

where the heat fluxes, f_i, are given by:

$$f_i = -k_{ij} T_{,j} \tag{62}$$

$$\nabla \cdot \bar{f} = -\frac{\partial}{\partial x} f_x - \frac{\partial}{\partial y} f_y - \frac{\partial}{\partial z} f_z = (k_{ij} T_{,j})_{,i} \tag{63}$$

and from Eq. (59), one may write

$$\int_V (k_{ij} T_{,j})_{,i} \, W \, dV = \int_S k_{ij} T_{,j} \nu_i \, W \, dS - \int_V k_{ij} T_{,j} W_{,i} dV \tag{64}$$

Substitution into Eq. (6) yields Eq. (7).

REFERENCES

1. Zienkiewicz. O.C., Jain, P.C., and Onate, E., "Flow of Solids During Forming and Extrusion: Some Aspects of Numerical Solutions," International Journal of Solids and Structures, Vol. 14, 1978, pp. 15-38
2. Altan, T., Lee, C.H., and Akgerman, N., "Approximate Calculation of Velocity and Temperature Distributions in Axisymmetric Extrusion and Drawing," Proceedings of the North American Metwalworking Research Conference: Metal Forming, Vol. 1, 1973, pp. 107-127.
3. Batra, R.C., "Cold Sheet Rolling, the Thermoviscoelastic Problem, A Numerical Solution," International Journal for Numerical Methods in Engineering, Vol. 11, 1977, pp. 671-682.
4. Nagpal, V., Lahoti, G.D,, and Altan, T., "A Numerical Method for Simultaneous Prediction of Metal Flow and Temperatures in Upset Forging of Rings," ASME publication, Paper No. 77-WA/PROD-35, 1977.
5. Lahoti, G.D., Shah, S.N., and Altan, T., "Computer-Aided Analysis of the Deformations and Temperatures in Strip Rolling", ASME publication, Paper No. 77-WA/PROD-34, 1977.
6. Webster, W.D., A Three-Dimensional Analysis of Extrusion and Metal Forming by the Finite Element Method, Doctoral dissertation, University of Missouri-Rolla, 1978.
7. Davidson, P. and Davis, R., "Mechanical Behavior of 6061-T651 Aluminum," AIAA Journal, Vol. 13, No. 12, 1975, pp. 1547-1548.
8. Conner, J.J., and Brebbia, C.A., Finite Element Techniques for Fluid Flow, 1st ed., Newnes-Butterworth, London, 1977, pp. 18-21.

9. Chacour, S., "'DANUTA', a Three-Dimensional Finite Element Program Used in the Analysis of Turbomachinery," ASME publication, Paper No. 71-WA/FE-29, 1971.

10. Zienkiewicz, O.C., Finite Element Method in Engineering Science, 2nd ed., McGraw-Hill, London, 1971.

11. Christie, I., et. al., "Finite Element Methods for Second Order Differential Equations with Significant First Derivatives," International Journal for Numerical Methods in Engineering, Vol. 10, 1976, pp. 1389-1396.

12. Heinrich, J.C., et. al., "An 'Upwind' Finite Element Scheme for Two-Dimensional Convective-Transport Equation," International Journal for Numerical Methods in Engineering, Vol. 11, 1977, pp. 131-143.

13. Heinrich, J.C. and Zienkiewicz, O.C., "Quadratic Finite Element Schemes for Two-Dimensional Convective-Transport Problems," International Journal for Numerical Methods in Engineering, Vol. 11, 1977, pp. 1831-1844.

14. Belytschko, T., Kennedy, J.M. and Schoeberle, D.F., "Quasi-Eulerian Finite Element Formulation for Fluid-Structure Interaction," ASME publication, Paper No. 78 PVP-60, 1978.

15. Dillard, D.A. and David, R.L., "Upwind Schemes for Three-Dimensional Quadratic Elements," International Journal for Numerical Methods in Engineering, submitted for publication.

16. Avitzur, B., Metal Forming: Processes and Analysis, McGraw-Hill, New York, 1968.

FIGURE CAPTIONS

Fig. 1 : Three-dimensional serendipity element in local coordinate system.

Fig. 2 : One-dimensional quadratic interpolation functions and the non-symmetric modifying function for the weight functions.

Fig. 3 : Three-dimensional Lagrangian element in local coordinate system.

Fig. 4 : Effect of upwinding on the numerical stability of the temperature distribution in a moving medium (one-dimensional geometry).

Fig. 5 : Profile view of an extrusion model.

Fig. 6 : An extrusion model - a quarter section of a round to round extrusion.

Fig. 7 : Comparison of numerical and analytic temperature predictions for extrusion ratio of 2.0 and various die angles.

Fig. 8 : Comparison of numerical and analytic temperature predictions for a die half angle of 30° and various extrusion ratios.

Fig. 9 : Effect of velocity on average temperature buildup for extrusion ratio of 2.0, die half angle of 30°.

Fig. 10: Isothermals for extrusion model.

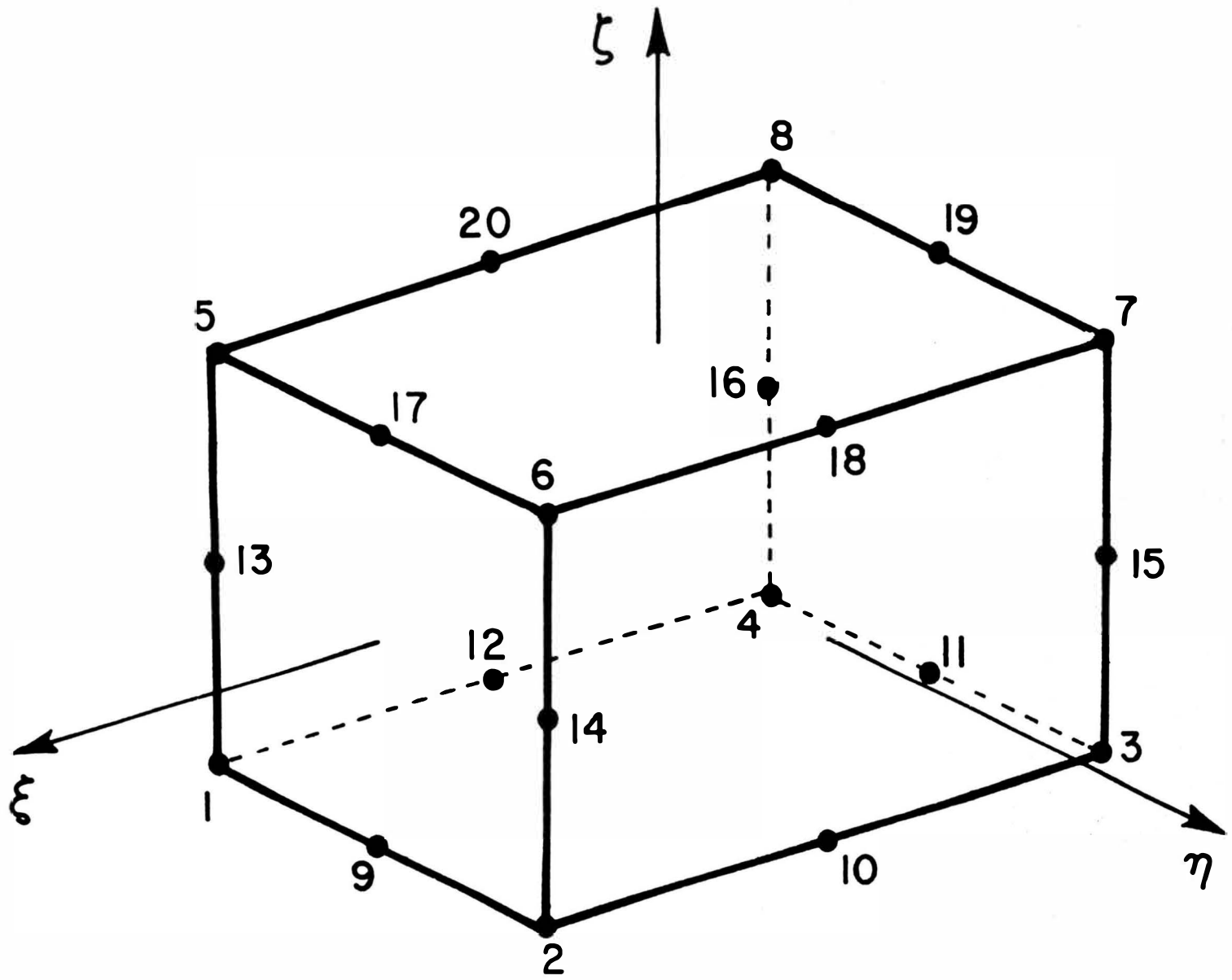

Figure 1

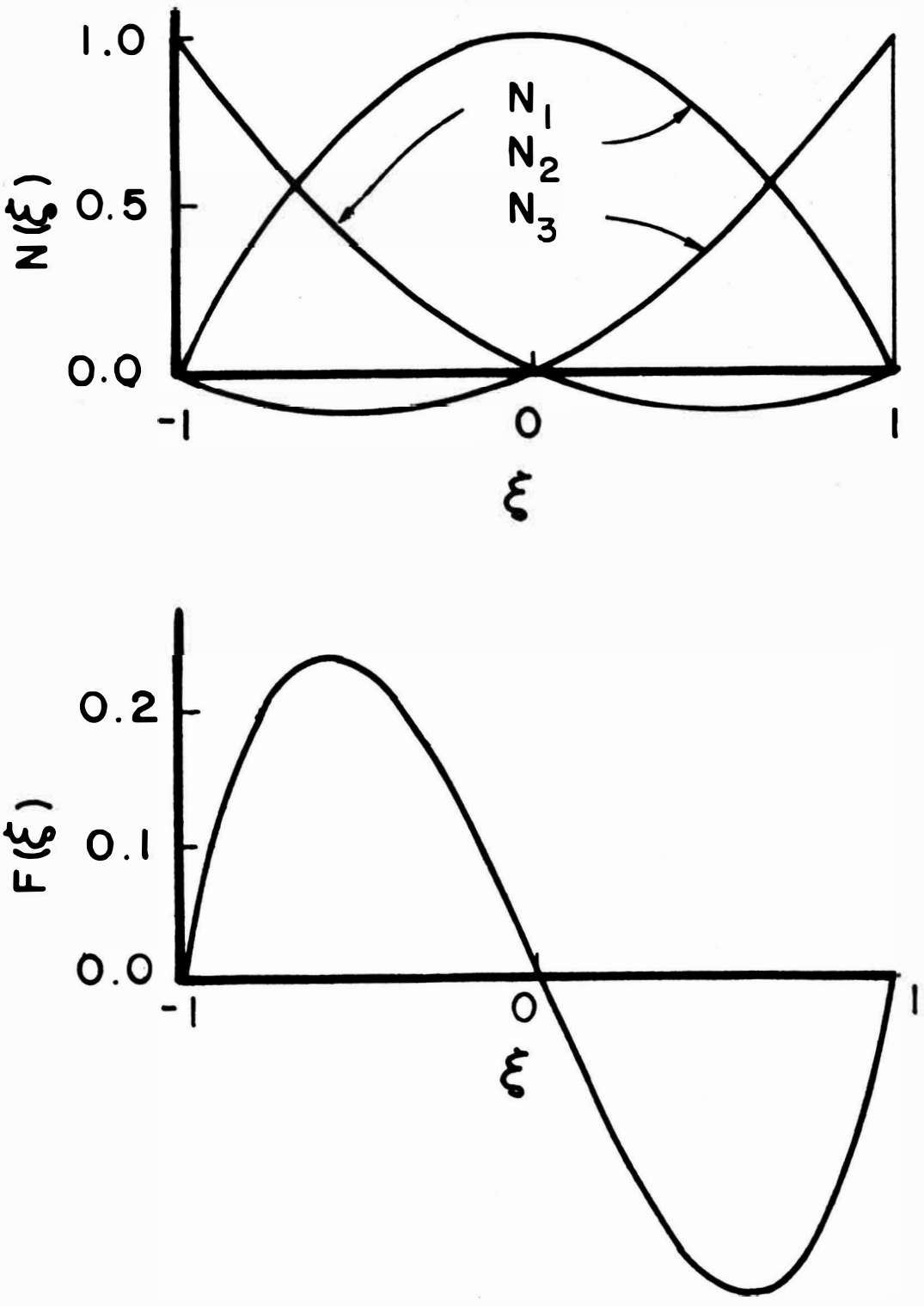

Figure 2

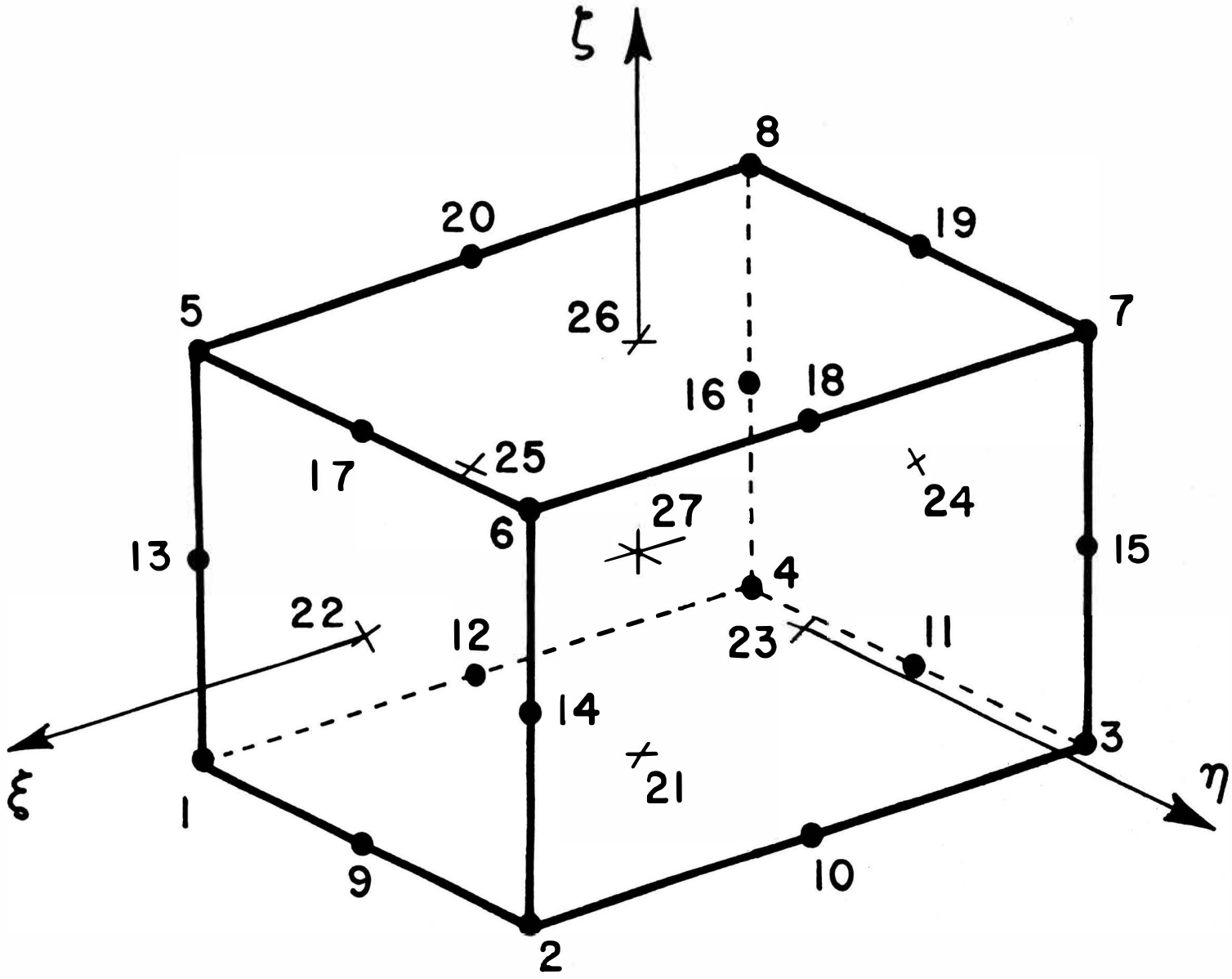

Figure 3

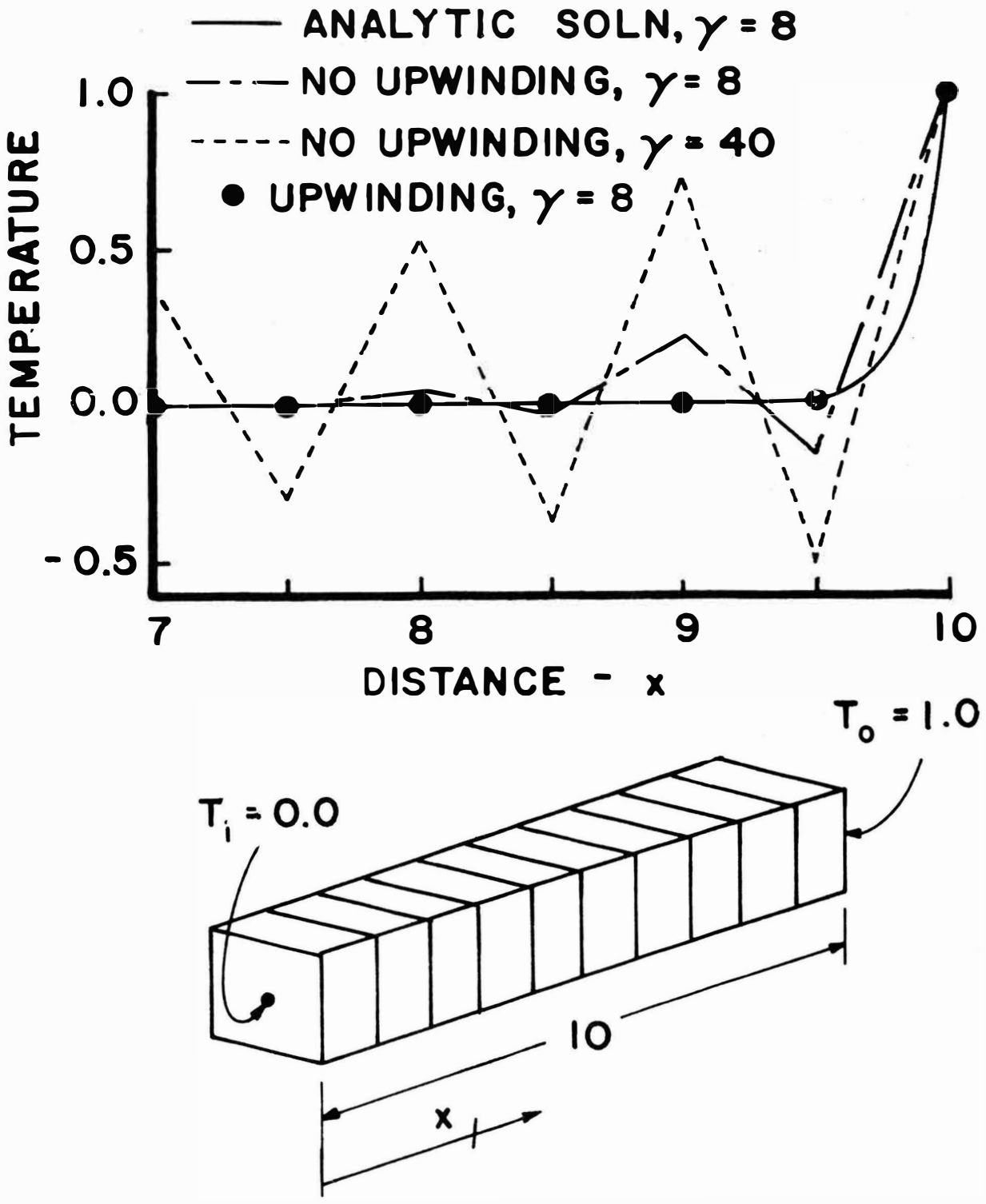
ANALYTIC SOLN, γ = 8
NO UPWINDING, γ = 8
NO UPWINDING, γ = 40
UPWINDING, γ = 8
TEMPERATURE
1.0
0.5
0.0
-0.5
7
8
9
10
DISTANCE - x
T₀ = 1.0
T₁ = 0.0
10
x

Figure 4

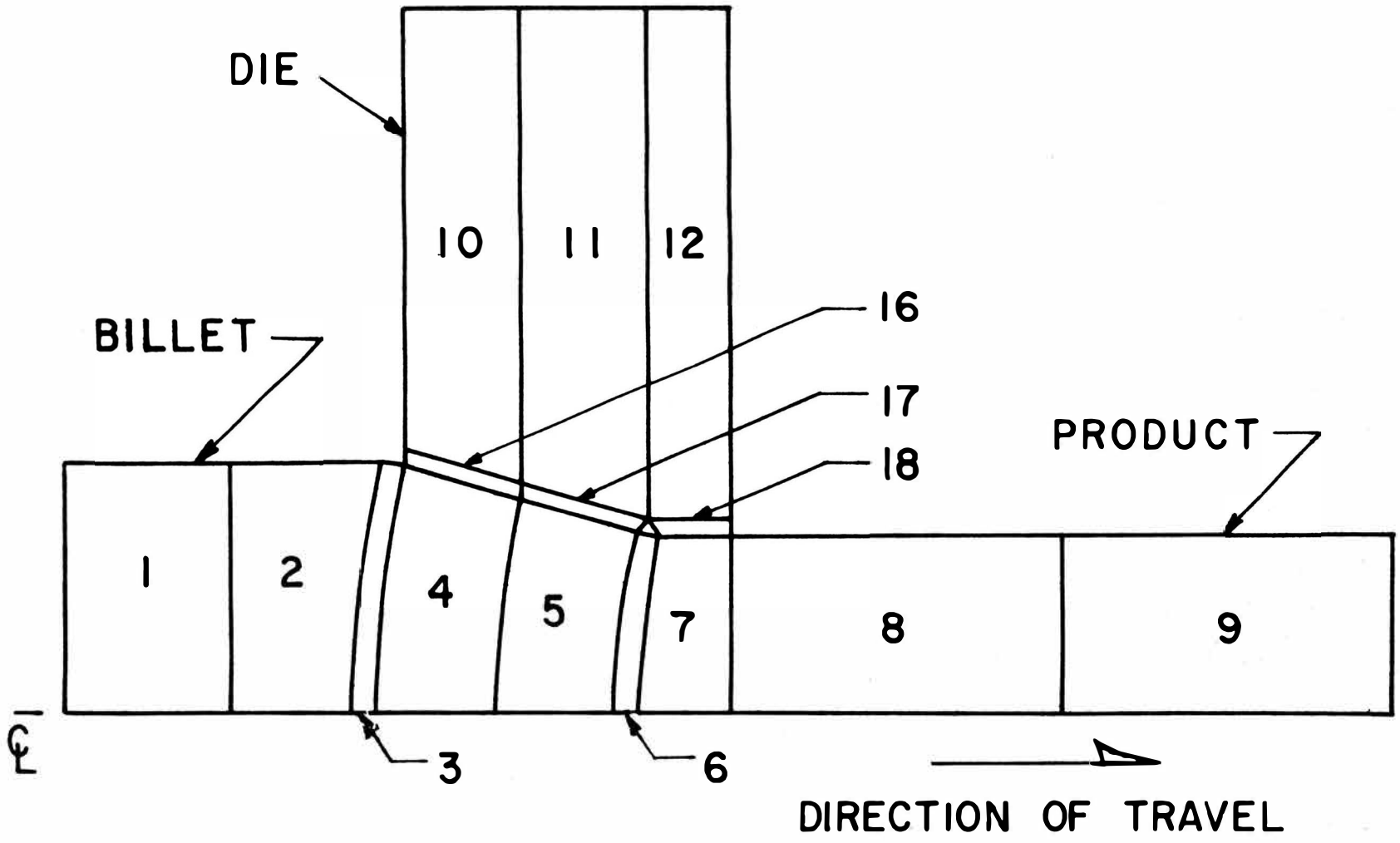
DIE
10
11
12
BILLET
16
17
18
PRODUCT
1
2
4
5
7
8
9
3
6
DIRECTION OF TRAVEL

Figure 5

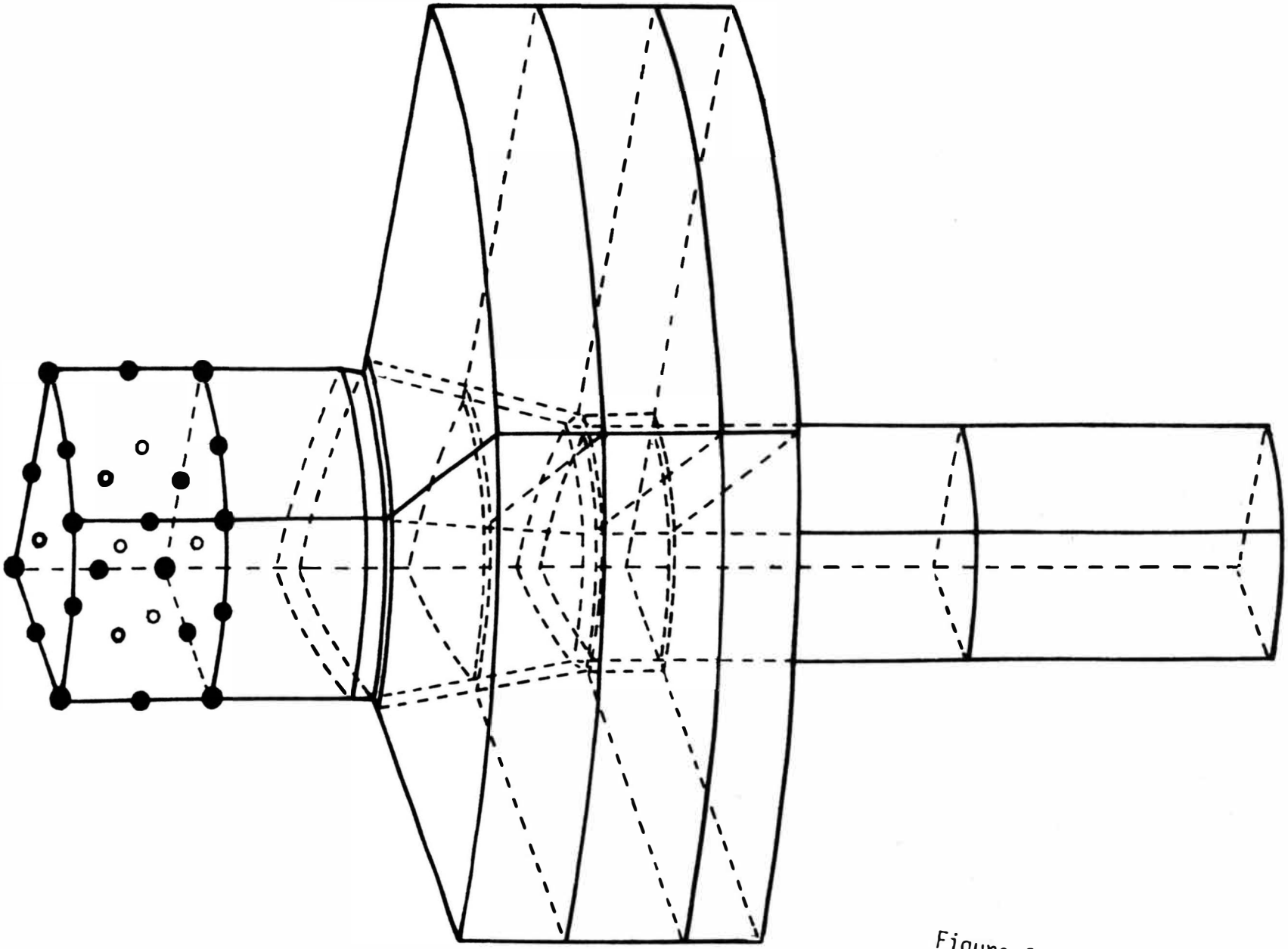

Figure 6

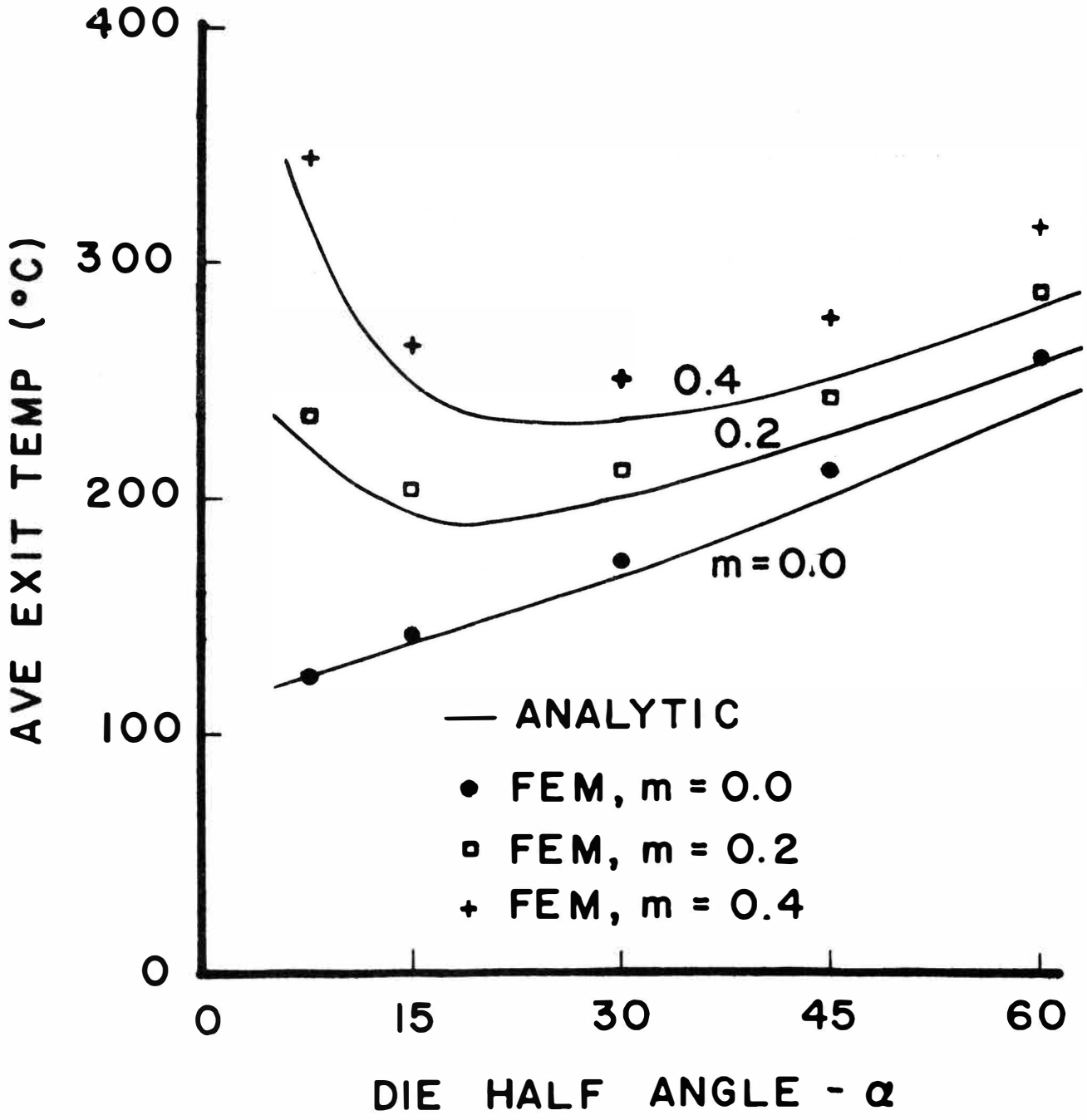
400
300
200
100
0
AVE EXIT TEMP (°C)
0.4
0.2
m = 0.0
— ANALYTIC
• FEM, m = 0.0
▫ FEM, m = 0.2
+ FEM, m = 0.4
0
15
30
45
60
DIE HALF ANGLE - α

Figure 7

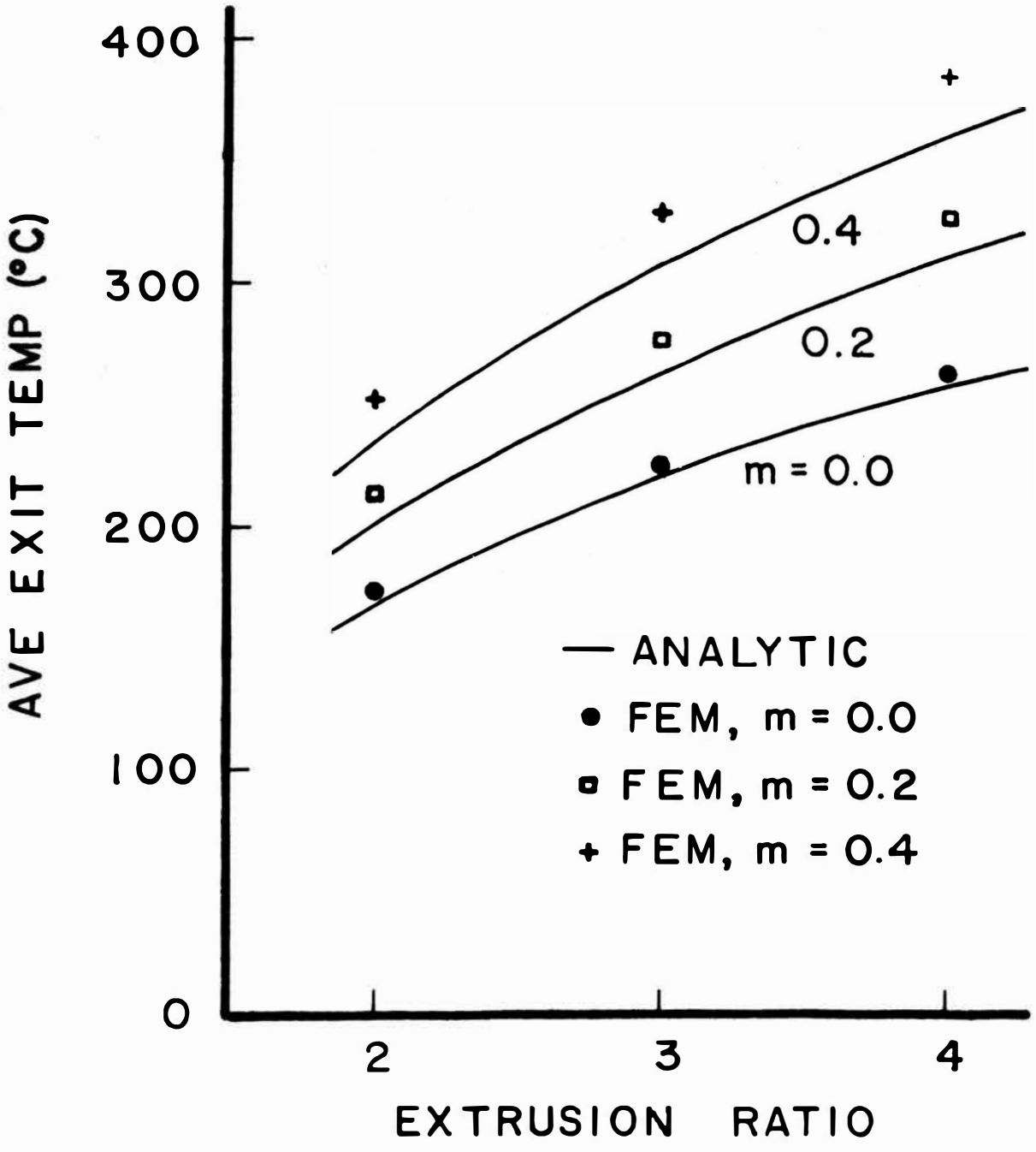
400
300
200
100
0
AVE EXIT TEMP (°C)
0.4
0.2
m = 0.0
— ANALYTIC
• FEM, m = 0.0
▫ FEM, m = 0.2
+ FEM, m = 0.4
2
3
4
EXTRUSION RATIO

Figure 8

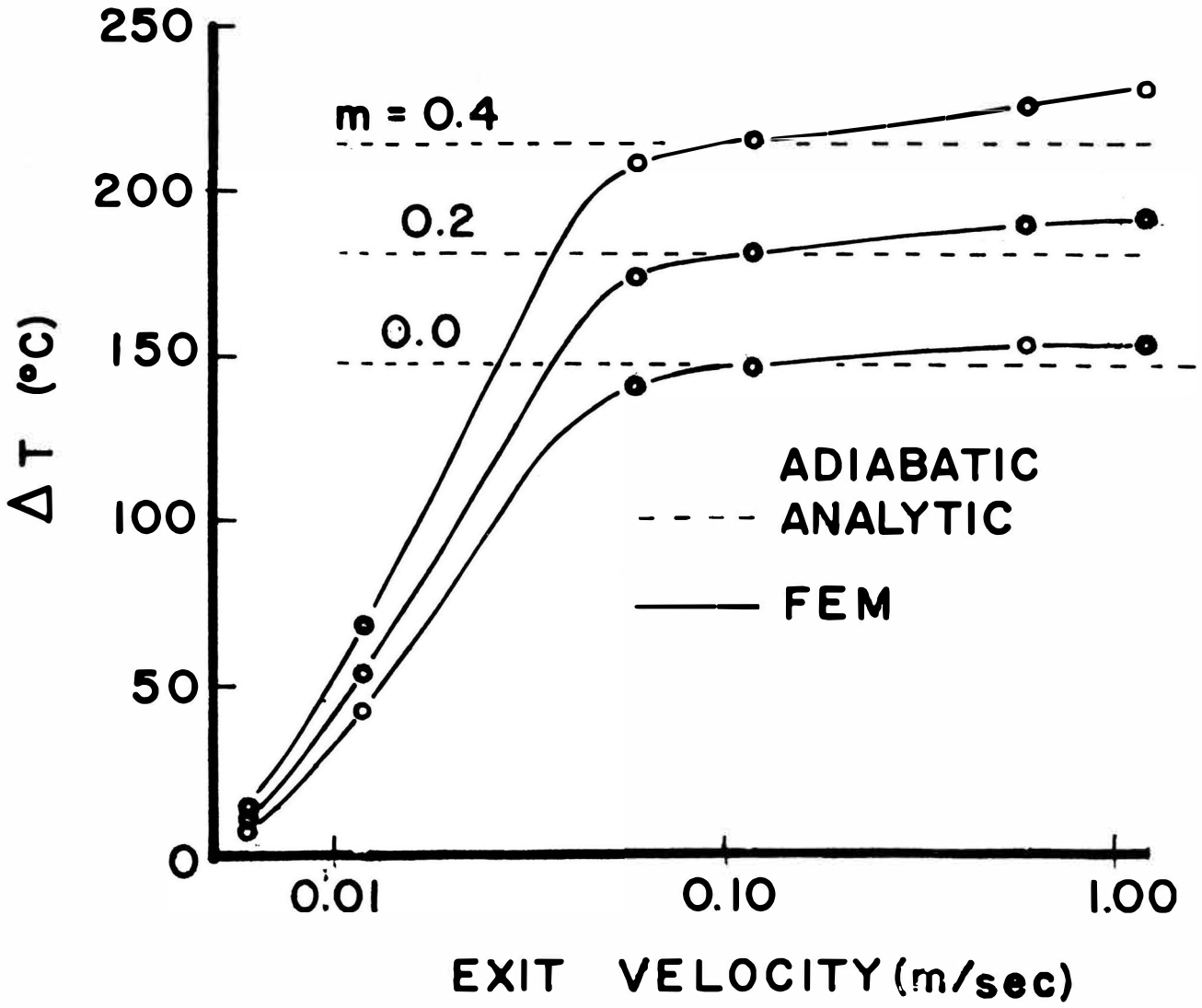
250
200
150
100
50
0
ΔT (°C)
m = 0.4
0.2
0.0
ADIABATIC
ANALYTIC
FEM
0.01
0.10
1.00
EXIT VELOCITY (m/sec)

Figure 9

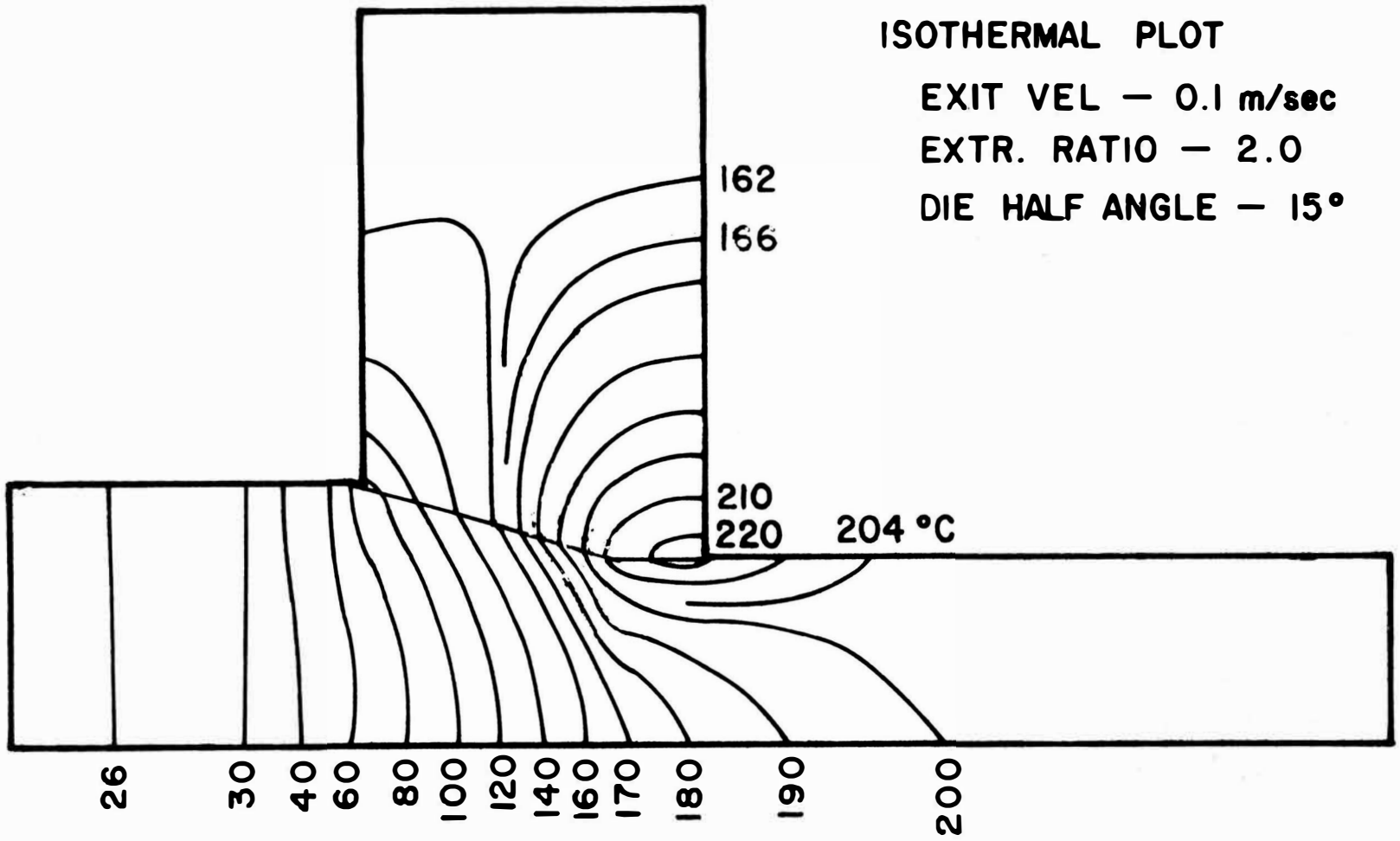
ISOTHERMAL PLOT
EXIT VEL — 0.1 m/sec
EXTR. RATIO — 2.0
DIE HALF ANGLE — 15°
162
166
210
220
204 °C
26
30
40
60
80
100
120
140
160
170
180
190
200

Figure 10

UPWIND SCHEMES FOR THREE-DIMENSIONAL QUADRATIC ELEMENTS

Prepared for

INTERNATIONAL JOURNAL OF NUMERICAL METHODS IN ENGINEERING

Written by

DAVID A. DILLARD AND ROBERT L. DAVIS

David A. Dillard
Graduate Student, Dept. of Engineering Mechanics
University of Missouri-Rolla
Rolla, MO

Robert L. Davis
Assistant Dean, School of Engineering
Professor, Dept. of Engineering Mechanics
University of Missouri-Rolla
Rolla, MO

SUMMARY

In solving the three-dimensional convective-transport equation, serious difficulties were encountered in applying upwind schemes to a quadratic, 20-degree of freedom, serendipity element. Inability to overcome these difficulties forced the adoption of a 27-degree of freedom, Lagrangian element to obtain acceptable solutions. Results using the Lagrangian element are compared with analytic solutions for several configurations.

INTRODUCTION

The presence of instabilities in the solutions of finite difference formulations of elliptic partial differential equations with significant first derivative terms has been recognized for some time. In recent years, similar difficulties have also been encountered in applications of the finite element technique to solve such equations. A method proposed by Bishop [1][1] for finite difference methods has been used successfully for determining temperature distributions in moving media [2, 3]. Allowing heat generation and transportation effects to be calculated for a small time step, followed by an equal time step in which only conduction takes place, effectively decouples the transportation and conduction terms and produces stable results. While the method is applicable to finite element formulations, it is undesirable for steady state analysis because of the computation time required for the iterative process envolved. For finite difference schemes, instabilities have also been avoided by using an upwind, rather than central difference stencil, for evaluation of the derivatives. Christie, Heinrick, et. al. [4-8] have applied similar upwind schemes to one- and two-dimensional finite element formulations, as well, and obtained good results.

The development of a finite element program for the analysis of general metal forming operations resulted in the need for a three-dimensional, quadratic thermal analysis element [9]. The thermal

---

[1] Numbers in brackets designate References at end of paper.

behavior of many metal forming operations is governed by the convective-transport equation. The use of standard Galerkin weight functions with a 20-degree of freedom, serendipity element for the thermal analysis produced unstable results above certain small velocities. Several techniques were tried for applying upwind schemes to this element, but no acceptable formulation was found. To obtain satisfactory solutions, a 27-degree of freedom, Lagrangian element was adopted for the analysis. The results obtained with the latter element are compared with closed form solutions for several configurations.

NUMERICAL FORMULATION

In the forming process of interest, the temperature field obeys the general form of the convective-transport equation:

$$\text{DE:} \quad \rho c\left(\frac{\partial T}{\partial t} + u_i T_{,i}\right) = \left(k_{ij} T_{,j}\right)_{,i} + Q \qquad \text{on } V \tag{1}$$

$$\text{BC:} \quad a_1 T + a_2 k_{ij} T_{,j} \nu_i = a_3 \qquad \text{on } S \tag{2}$$

$$\text{IC:} \quad T = T_o(x, y, z) \text{ at } t = 0 \qquad \text{on } V \tag{3}$$

where ρ is the density; c, the specific heat; u_i, the velocity components; T, the temperature; k_{ij} $(=k_{ji})$, the thermal conductivities; Q, the heat generation; V, the body being considered; a_1, a_2, and a_3 are known functions describing the boundary conditions; ν_i, the direction cosines of a vector normal to dS; and S is the surface of the body. For convenience, let

$$\Omega = a_1/a_2 \tag{4}$$

$$\Psi = a_3/a_2 \tag{5}$$

An application of the weighted residual technique [10] to the governing equations (1) and (2) yields

$$\int_V \left[\rho c\left(\frac{\partial T}{\partial t} + u_i T_{,i}\right) - \left(k_{ij} T_{,j}\right)_{,i} - Q\right] W dV + \int_S \left[k_{ij} T_{,j} \nu_i + (\Omega T - \Psi)\right] W dS = 0 \tag{6}$$

where T is assumed to satisfy the essential boundary conditions, and W is some appropriately chosen weight function. The divergence theorem allows one to write

$$\int_V \{[\rho c(\frac{\partial T}{\partial t} + u_i T_{,i}) - Q] W + k_{ij} T_{,j} W_{,i}\} \, dV + \int_S (\Omega T - \Psi) W dS = 0 \tag{7}$$

For the special case of the boundary condition, equation (2), in which $a_2 \to 0$, Ω and Ψ will dominate the residual statement. Indeed, in the limit, the residual statement reduces to

$$\Omega T - \Psi = 0 \tag{8}$$

The temperature is taken as

$$T = \{\phi\}^T \{T^n\} \qquad \phi_i = \phi_i(x, y, z) \tag{9}$$

and the weight as

$$W = \{\chi\}^T \{\delta T^n\} \qquad \chi_i = \chi_i(x, y, z) \tag{10}$$

where $\{\delta T^n\}$ is the vector of arbitrary virtual increments of temperature at each node. Substituting these into the weighted residual statement results in the classical system of equations given by

$$\bar{C} \{\partial T^n/\partial t\} + \bar{H} \{T^n\} = \{F\} \tag{11}$$

where

$$\tilde{C} = \int_V \rho c \{\chi\} \{\phi\}^T \, dV \tag{12}$$

$$\tilde{H} = \int_V \rho c u_i \{\chi\} \{\phi_{,i}\}^T \, dV + \int_V k_{ij} \{\chi_{,i}\} \{\phi_{,j}\}^T \, dV + \int_S \Omega \{\chi\} \{\phi\}^T \, dS \tag{13}$$

$$\{F\} = \int_V Q \{\chi\} \, dV + \int_S \Psi \{\chi\} \, dS \tag{14}$$

For the purpose of this paper only the steady state solution will be considered, reducing the system of equations to

$$\tilde{H} \{T^n\} = \{F\} \tag{15}$$

Early investigation proceeded with the use of a 20-node, quadratic, isoparametric element. Standard Galerkin weight functions resulted in instabilities in the solution when the velocity exceeded some small value. Stable results could be obtained only for velocities several orders of magnitude smaller than those of interest for high speed drawing operations.

THE UPWINDING TECHNIQUE

Consider a one-dimensional, quadratic element with standard parabolic interpolation functions given by

$$N_1(\xi) = 1/2\ \xi(\xi - 1) \qquad -1 \leq \xi \leq 1 \tag{16}$$

$$N_2(\xi) = 1 - \xi^2 \tag{17}$$

$$N_3(\xi) = 1/2\ \xi(\xi + 1) \tag{18}$$

If a local or element Peclet number is defined as

$$\gamma = \left| \frac{uh}{\kappa} \right| \tag{19}$$

where $\kappa = k/\rho c$; u, the velocity along the element and h is the length of the element, instabilities are predicted when this local Peclet number exceeds a value of 4.0 for any given element. To suppress the instabilities, Heinrich and Zienkiewicz [6] have proposed the use of non-symmetric weighting functions given by

$$W_1 = W_1(\xi, \alpha) = N_1(\xi) - \alpha F(\xi) \tag{20}$$

$$W_2 = W_2(\xi, \beta) = N_2(\xi) + 4\beta F(\xi) \tag{21}$$

$$W_3 = W_3(\xi, \alpha) = N_3(\xi) - \alpha F(\xi) \tag{22}$$

where

$$F(\xi) = 5/8\ \xi(\xi - 1)(\xi + 1) \tag{23}$$

and α and β are parameters which control the amount of upwinding.

For the case of no heat generation (Q = 0), constant velocity, regular mesh size of h, and specified temperature boundary conditions, Heinrich shows that there are optimal values of α and β which, when used in the weight function, will reproduce the exact solution at each node. These optimal values of the upwinding parameters are

$$\beta_o = \coth\left(\frac{\gamma}{4}\right) - 4/\gamma \tag{24}$$

$$\alpha_o = 2 \tanh\left(\frac{\gamma}{2}\right)\left(1 + \frac{3\beta_o}{\gamma} + \frac{12}{\gamma^2}\right) - \frac{12}{\gamma} - \beta_o \tag{25}$$

As the velocity becomes large, α_o and β_o both approach a value of 1. Fig. 1 illustrates the shape of the proposed weighting functions for $\alpha_o = \beta_o = 1$.

Finally, Heinrich extends these one-dimensional weights to two-dimensional Lagrangian (9 node) and serendipity (8 node) elements. He concludes that the Lagrangian element performs better in certain applications, although it is implied that both elements give acceptable results.

THE THREE-DIMENSIONAL LAGRANGIAN ELEMENT

The extension of the one-dimensional weight functions to two and three dimensions is quite straightforward for the Lagrangian element. The combined weight is expressed simply as the product of one-dimensional weights along each coordinate axis, just as the Lagrangian interpolation functions are products of one-dimensional interpolation functions.

For the three-dimensional Lagrangian element shown in Fig. 2, the interpolation functions are

$$\phi_{ijk}(\xi, \eta, \zeta) = N_i(\xi)\, N_j(\eta)\, N_k(\zeta) \tag{26}$$

and the weight functions are

$$\chi_{ijk}(\xi, \eta, \zeta) = W_i(\xi, \alpha^i, \beta^i)\, W_j(\eta, \alpha^j, \beta^j)\, W_k(\zeta, \alpha^k, \beta^k) \tag{27}$$

where α^i and β^i are the optimal upwind parameters for the line passing through the node and parallel to the ξ-axis, etc. A set of these parameters (α_o and β_o) is defined for 27 lines: 9 for $\xi = \pm 1, 0$ and $\eta = \pm 1, 0$; 9 for $\xi = \pm 1, 0$ and $\zeta = \pm 1, 0$; and 9 for $\eta = \pm 1, 0$ and $\zeta = \pm 1, 0$.

Indeed, the Lagrangian element permits a very simple blending of the one-dimensional weights throughout several dimensions. The element appears to perform very well; some results are given later.

THE THREE-DIMENSIONAL SERENDIPITY ELEMENT

Unlike the convenient extension of upwinding to the Lagrangian element, the blending of one-dimensional weights throughout the three-dimensional serendipity element shown in Fig. 3 is not trival. If linear interpolation functions are defined as

$$L_1(\xi) = 1/2(1 - \xi) \qquad -1 \leq \xi \leq 1 \tag{28}$$

$$L_3(\xi) = 1/2(1 + \xi) \tag{29}$$

the interpolation functions of the three-dimensional serendipity element for a corner node may be expressed as

$$\phi = N_i(\xi)\, L_j(\eta)\, L_k(\zeta) + L_i(\xi)\, N_j(\eta)\, L_k(\zeta) + L_i(\xi)\, L_j(\eta)\, N_k(\zeta) - 2\, L_i(\xi)\, L_j(\eta)\, L_k(\zeta) \tag{30}$$

Replacing N_ℓ with W_ℓ appears to be an adequate means of mapping the modified weighting functions throughout the element. The midside nodes, however, are of the form:

$$\phi = N_2(\xi)\, L_j(\eta)\, L_k(\zeta) \qquad \text{for an } i = 2 \text{ node} \tag{31}$$

Consistency with the corner node mapping would suggest replacing N_2 with W_2. Indeed, this seems to be the three-dimensional version of the form proposed by Heinrich.

Suppose there is only one component of velocity in local coordinates, and that it is along the ξ-axis. Note that while the weight for all the corner nodes is affected by this velocity, the

weight functions of midside nodes on axes parallel to η and ζ are not affected by this velocity. Thus the weighting function for these nodes would be the same as the interpolation functions. One might predict instabilities from the use of Galerkin weights for some nodes, and indeed, this is what the program reveals. Because all nodes are coupled, instabilities induced by these nodes causes the results to be unacceptable.

Apparently, the serendipity family of elements, so named because the interpolation functions must be derived by inspection rather than a mathematically systematic formulation [11], does not lend itself to upwinding as easily as the Lagrangian family elements. Other blending procedures, which cause the weighting functions of all nodes to be affected by all velocity components, were postulated by inspection and studied. The most promising and systematic approach involved weighting functions given by

$$\chi_{ijk}(\xi, \eta, \zeta) = W_i(\xi)\, P_j(\eta)\, P_k(\zeta) \tag{32}$$

$$+ P_i(\xi)\, W_j(\eta)\, P_k(\zeta) + P_i(\xi)\, P_j(\eta)\, W_k(\zeta)$$

$$- 2\, P_i(\xi)\, P_j(\eta)\, P_k(\zeta)$$

for all 20 nodes. The blending functions, P_m, could be chosen as any appropriate functions. Note that unlike the weights for the Lagrangian element, these weights, in general, will be different from the interpolation functions even for the stationary case. Note, however, that if

$$P_1(\xi) = 1/2(1 - \xi) \tag{33}$$

$$P_2(\xi) = 0 \tag{34}$$

$$P_3(\xi) = 1/2(1 + \xi) \tag{35}$$

the resulting weights are identical to that of equations (30) and (31). Several sets of blending functions comprised of various combinations of linear, bilinear, and quadratic functions were studied. The quadratic blending functions given by

$$P_i = N_i \tag{36}$$

produced the only acceptable results. Although the resultant solutions for a two element model of a one-dimensional rod problem produced excellent agreement with the exact solutions for a variety of end boundary conditions, internal heat generation, and velocities, the solutions were erroneous for two- and three-dimensional configurations. Examination of the $\tilde{H}$ matrix for an element revealed that some of the influence coefficients between nodes in the same element are zero. This implied that the temperature at some nodes is independent of the temperature at other nodes within the same element. The element was deemed unsatisfactory on these grounds.

It is interesting to note that these zero terms occur only between nodes on different faces of the hexahedron. It is, therefore, possible that a two-dimensional element utilizing these quadratic blending functions might yield acceptable results.

RESULTS

A comparison of the linear blending of the weights as given by Eqs. (30) and (31) and the quadratic blending as given by Eqs. (32) and (36) was made for the serendipity element in Fig. 4. A two element model with specified temperatures on the end faces and insulated sides was used for the comparison. The quadratic blending method yielded eight digit agreement with the analytic solution for various velocities for this one-dimensional configuration.

The expressions for α_o and β_o were derived for the case of no heat generation, uniform mesh size, constant velocity, and specified temperature boundary conditions. The Lagrangian element performed very well even when these restrictions were violated. Using a two element model with insulated sides, results were obtained for one-dimensional configurations. Fig. 5 illustrates the effect of uniform heat generation throughout the elements. The heat generation was given as proportional to the velocity. The numerical solutions agreed to eight digits with the analytic solution.

Figs. 6 and 7 show the results obtained with non-uniform mesh size. The ratios of mesh lengths are in 4:1 and 1:4, respectively. The large element upstream results showed less than a percent error with the exact solution; the large element downstream results agreed to four digits. The use of a specified flux boundary condition on an end face was also investigated. The results are shown in Table 1. The positive local Paclet numbers correspond to a specified flux at the outlet; the results are in very good agreement with the analytic solution. The negative Peclet numbers correspond to a specified flux at the inlet.

While the results are good for small velocities, they do not converge to the exact solution for high velocities. Because of the upwinding nature of the solution scheme, the essential boundary condition should always be enforced at the furthest upstream nodes to ensure convergence with the correct solution.

The element has also been used for several two- and three-dimensional problems. A coarse grid was used to model a round to round extrusion process. The results agree very well with the thermal buildups predicted by analytic integration of the power of deformation for the specified velocity field. Details of this analysis have been presented elsewhere [9].

CONCLUDING REMARKS

Upwind schemes have been successfully applied to a three-dimensional, quadratic Lagrangian element for the solution of the convective-transport equation. The authors were not able to overcome the difficulties encountered in applying upwind schemes to the three-dimensional serendipity element originally under investigation.

The governing differential equation predicts very large temperature gradients in a fast moving medium where there is a significant heat flux passing through an element surface. Because these gradients are typically much steeper than those encountered in elasticity problems, care should be exercised to provide an appropriate grid in such regions.

When used in connection with a flow analysis program, the authors feel that the element described herein is quite adequate for the thermal analysis of general metal forming operations. It is also felt that the element may be useful in other areas of engineering interest.

TABLE 1

COMPARISON OF ANALYTIC AND NUMERICAL SOLUTIONS FOR A MOVING MEDIA WITH A SPECIFIED FLUX BOUNDARY CONDITION ON ONE END. T = 1.0 WAS SPECIFIED ON THE OTHER END.

	X = L/2		X = 3L/4		X = L	
	Numerical	Analytic	Numerical	Analytic	Numerical	Analytic
1.0	1.0775	1.0775	1.1571	1.1571	1.2883	1.2882
5.0	1.0004	1.0004	1.0057	1.0055	1.0700	1.0667
50.0	1.0000	1.0000	1.0000	1.0000	1.0094	1.0067
- 1.0	2.5574	2.5569	2.9140	2.9134	313.03	312.97
- 5.0	1532.10	1459.54	1541.64	1468.62	1542.42	1469.36

REFERENCES

1. Bishop, J.F.W., "An Approximate Method for Determining the Temperature Reached in Steady-State Problems of Plane Plastic Strain", Quarterly Journal of Mechanics and Applied Mathematics, Vol. 9, 1956, p. 236.
2. Altan, T., Lee, C.H., and Akgerman, N., "Approximate Calculation of Velocity and Temperature Distributions in Axisymmetric Extrusion and Drawing", Proceedings of the North American Metal Working Research Conference: Metal Forming, Vol. 1, 1973, pp. 107-127.
3. Lahoti, G.D., Shah, S.N., and Altan, T., "Computer-Aided Analysis of the Deformations and Temperatures in Strip Rolling", ASME publication, Paper No. 77-WA/PROD-34, 1977.
4. Christie, I., et. al., "Finite Element Methods for Second Order Differential Equations with Significant First Derivatives", International Journal for Numerical Methods in Engineering, Vol. 10, 1976, pp. 1389-1396.
5. Heinrich, J.C., et. al., "An 'Upwind' Finite Element Scheme for Two-Dimensional Convective Transport Equation", International Journal for Numerical Methods in Engineering, Vol. 11, 1977, pp. 131-143
6. Heinrich, J.C., and Zienkiewicz, O.C., "Quadratic Finite Element Schemes for Two-Dimensional Convective-Transport Problems", International Journal for Numerical Methods in Engineering, Vol. 11, 1977, pp. 1831-1844.

7. Zienkiewicz, O.C., Jain, P.C., and Oñate, E., "Flow of Solids During Forming and Extrusion: Some Aspects of Numerical Solutions", International Journal of Solids and Structures, Vol. 14, 1978, pp. 15-38.

8. Belytschko, T., Kennedy, J.M., and Schoeberle, D., "Quasi-Eulerian Finite Formulation for Fluid-Structure Interaction", ASME Publication, Paper No. 78 PVP-60, 1978.

9. Dillard, D.A., and Davis, R.L., "A Quadratic Finite Element for the Three-Dimensional Convective-Transport Equation", submitted to ASME for publication.

10. Conner, J.J., and Brebbia, C.A., Finite Element Techniques for Fluid Flow, 1st ed., Newnes-Butterworth, London, 1977, pp. 18-21.

11. Zienkiewicz, O.C., Finite Element Method in Engineering Science, 2nd ed., McGraw-Hill, London, 1971.

12. Avitzur, B., Metal Forming: Processes and Analysis, McGraw-Hill, New York, 1968.

FIGURE CAPTIONS

Fig. 1: Modified weight functions for node i, $\alpha = \beta = 1$.

Fig. 2: Lagrangian element in local coordinates.

Fig. 3: Serendipity element in local coordinates.

Fig. 4: Comparison of linear and quadratic blending for weights in serendipity element for $\gamma = 50$.

Fig. 5: Temperature distribution in moving media with homegeneous heat generation.

Fig. 6: Temperature profiles - Mesh ratio 4:1

Fig. 7: Temperature profiles - Mesh ratio 1:4

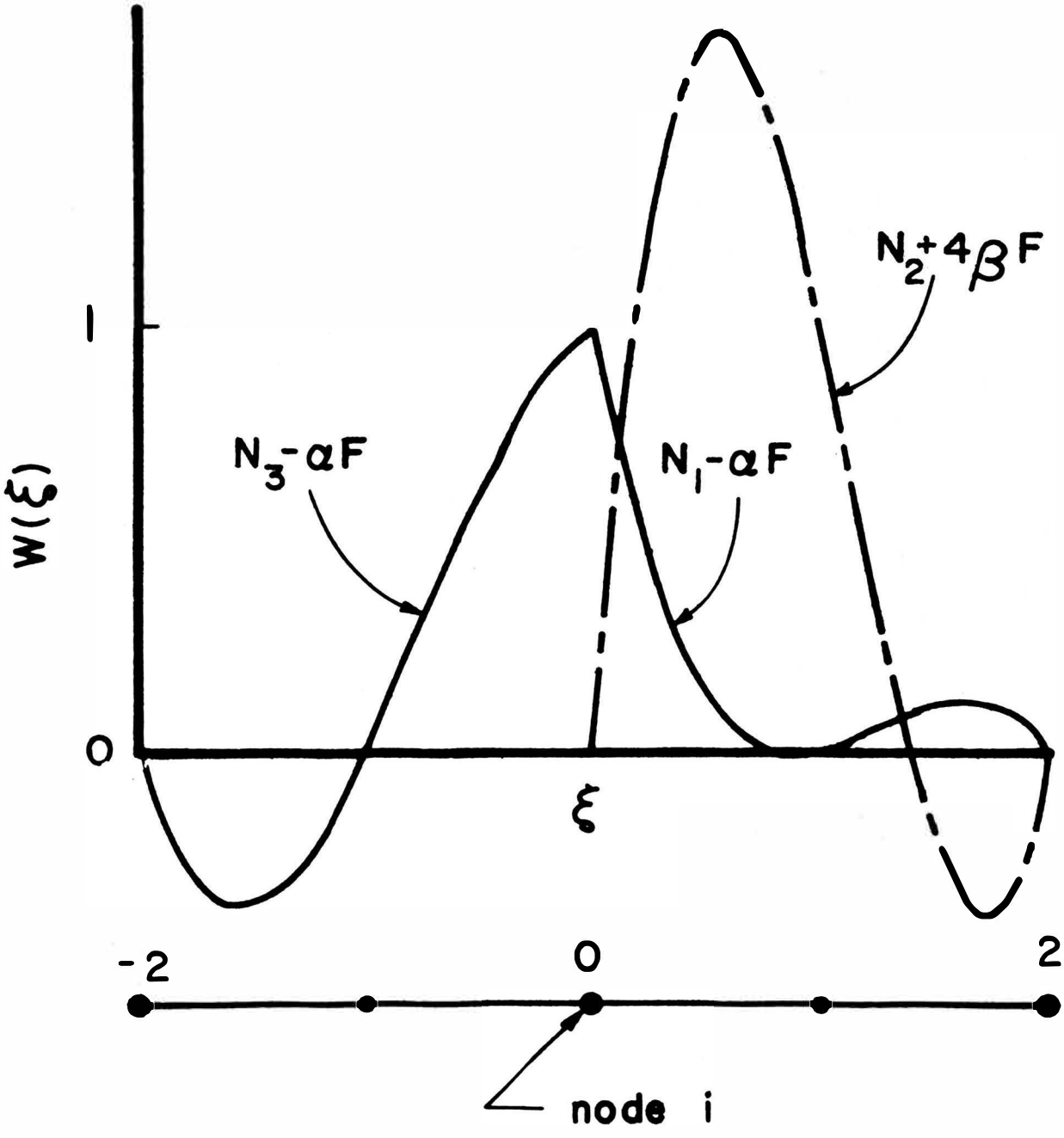

Figure 1

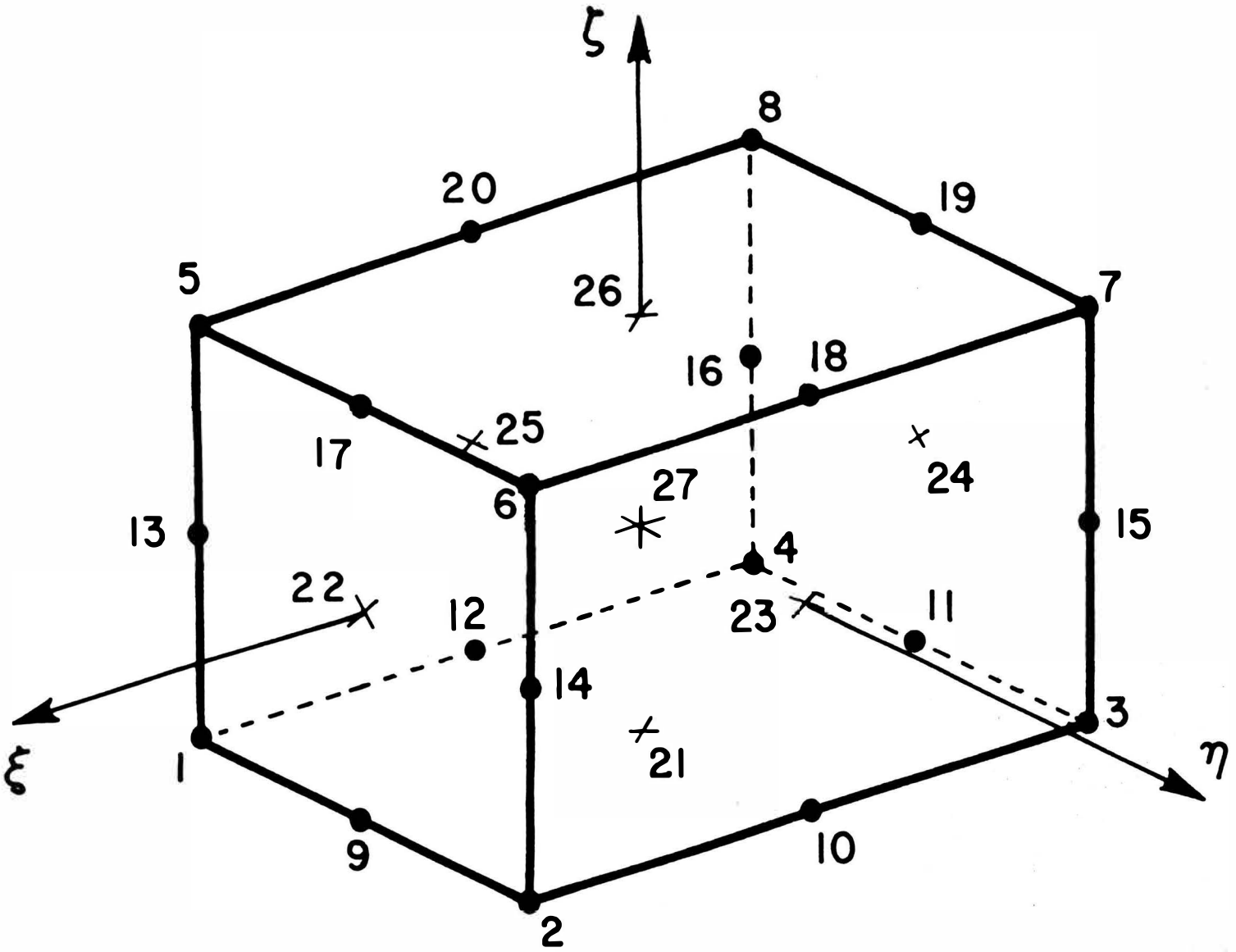

Figure 2

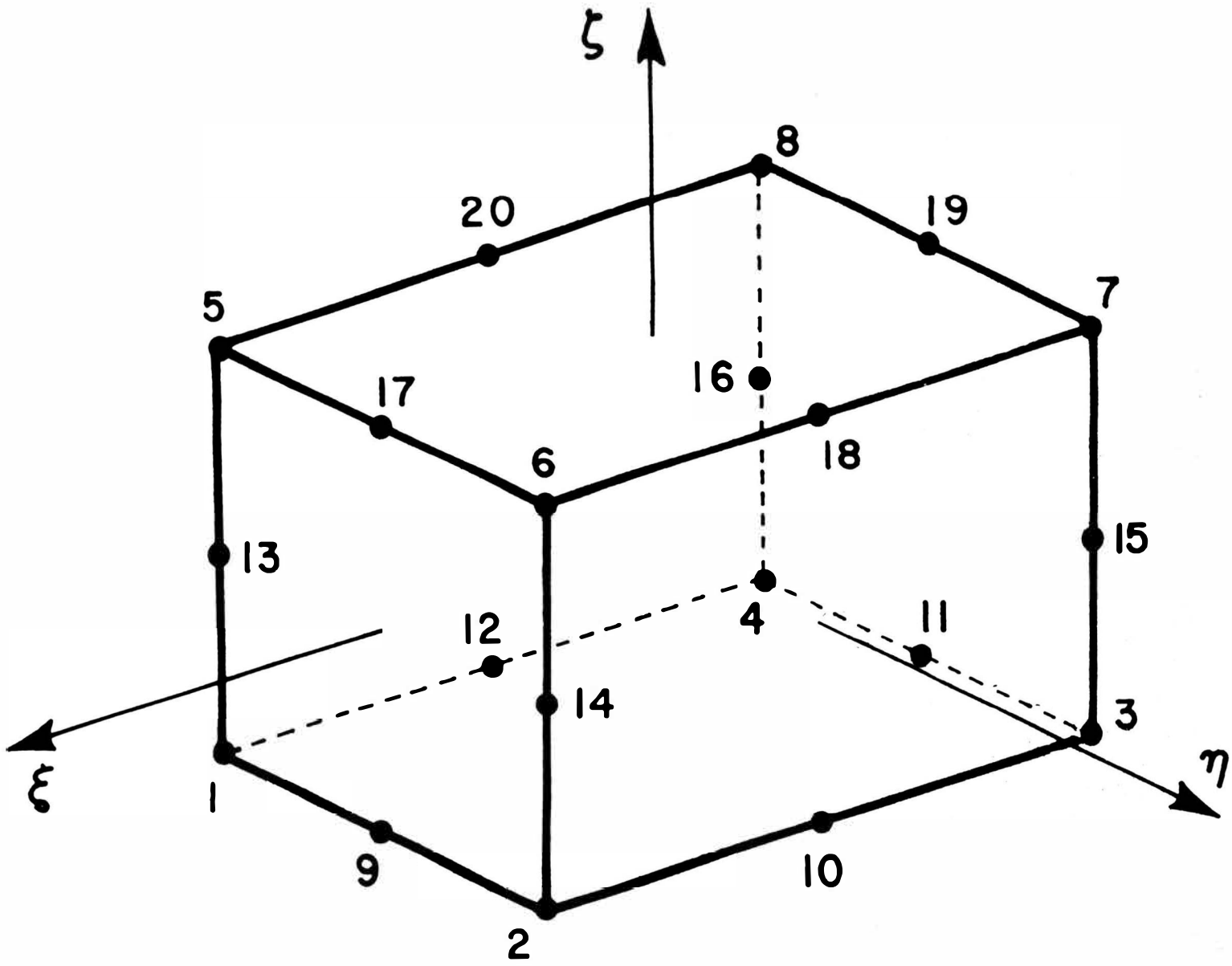

Figure 3

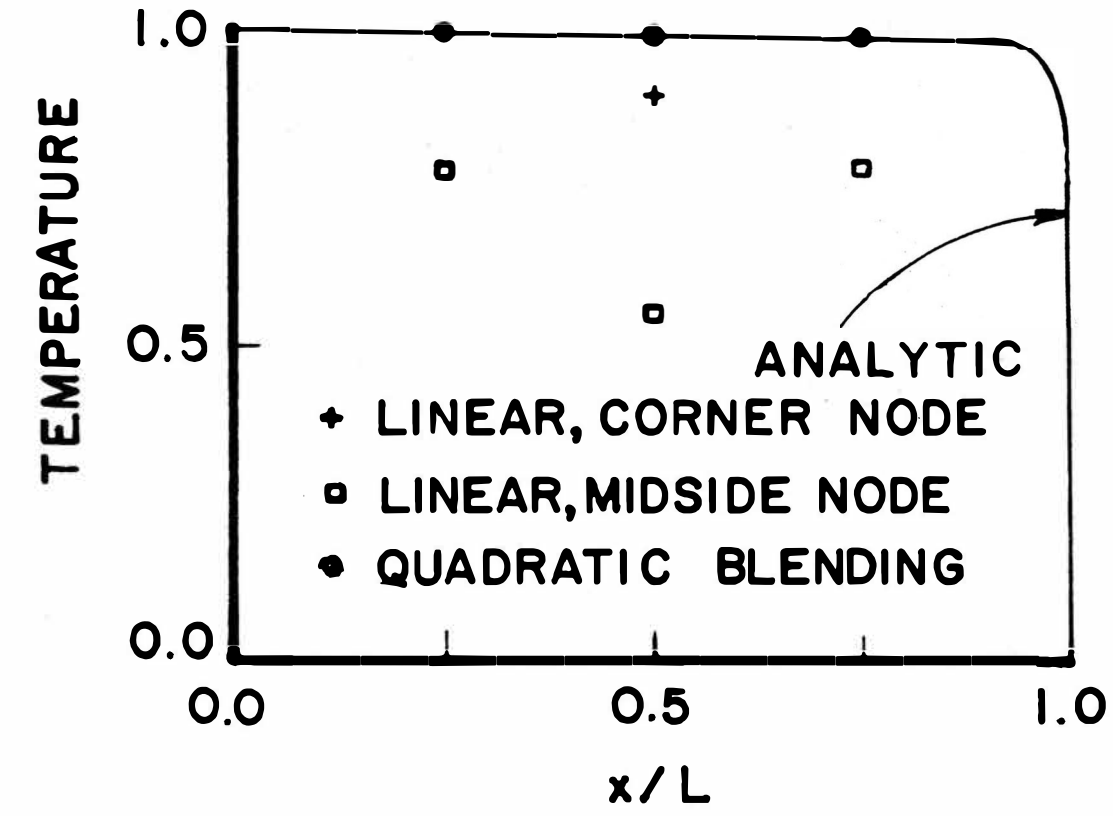
1.0
0.5
0.0
TEMPERATURE
ANALYTIC
LINEAR, CORNER NODE
LINEAR, MIDSIDE NODE
QUADRATIC BLENDING
0.0
0.5
1.0
x/L

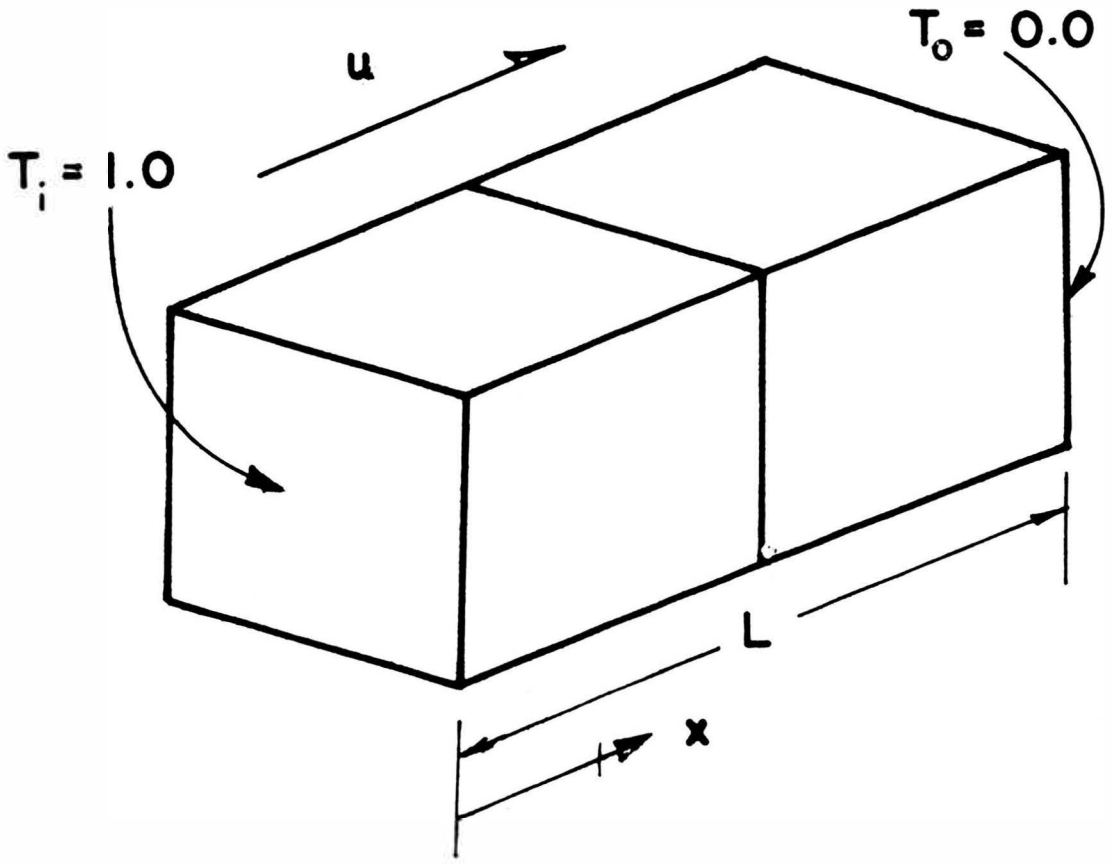
u
T_i = 1.0
T_o = 0.0
L
x

Figure 4

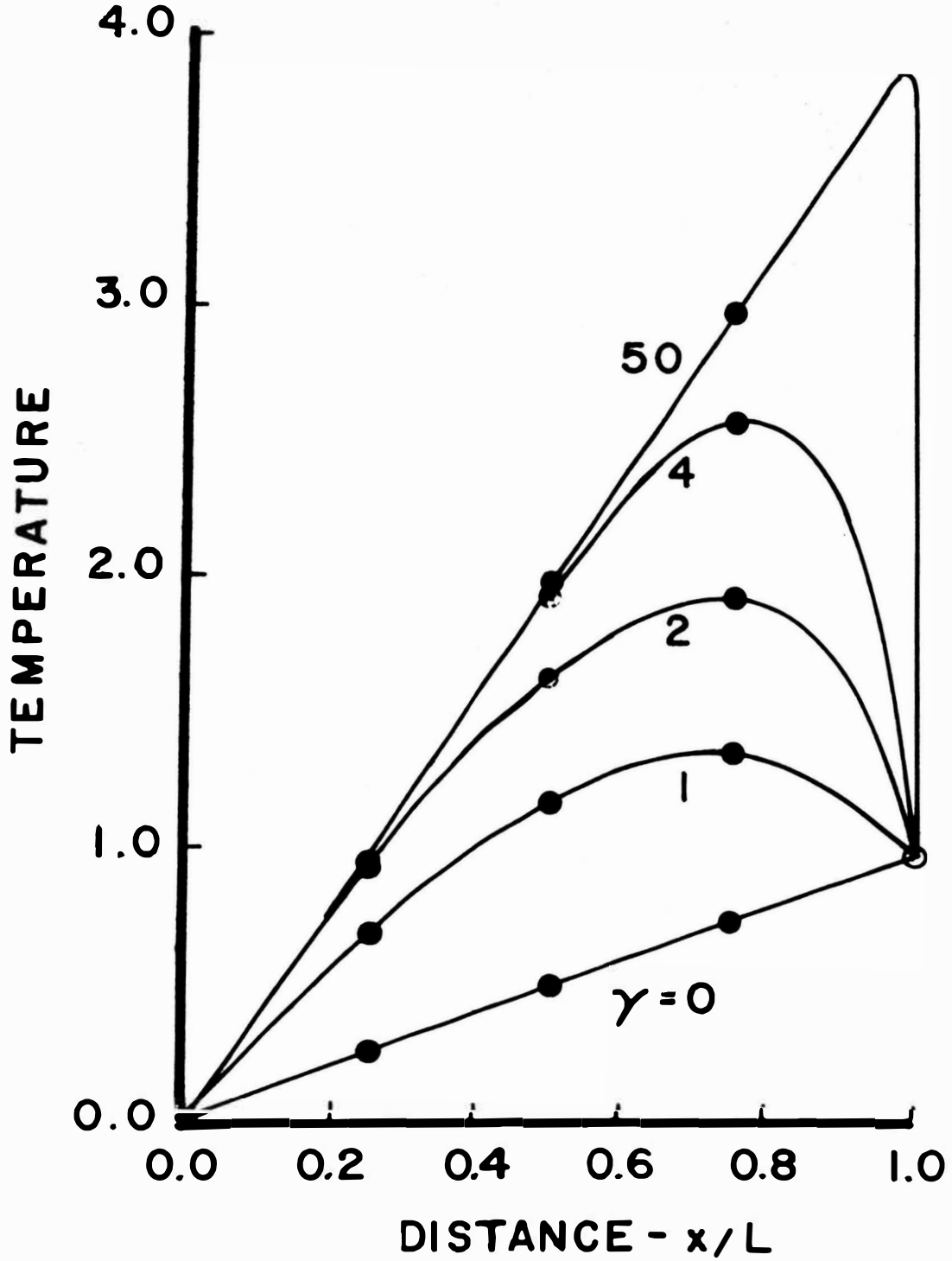
4.0
3.0
2.0
1.0
0.0
TEMPERATURE
50
4
2
1
γ=0
0.0
0.2
0.4
0.6
0.8
1.0
DISTANCE - x/L

Figure 5

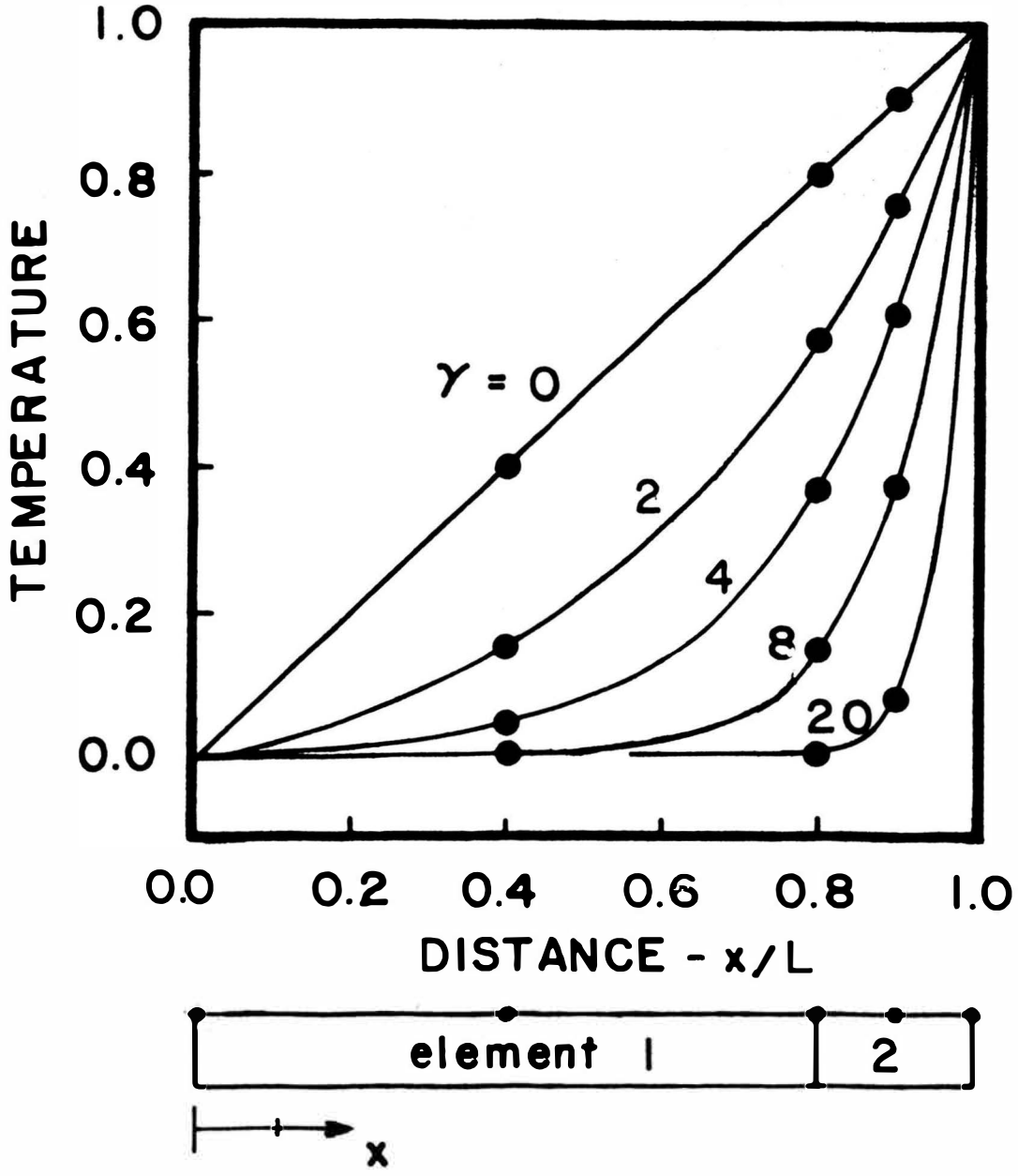
1.0
0.8
0.6
0.4
0.2
0.0
TEMPERATURE
γ = 0
2
4
8
20
0.0
0.2
0.4
0.6
0.8
1.0
DISTANCE - x/L
element 1
2
x

Figure 6

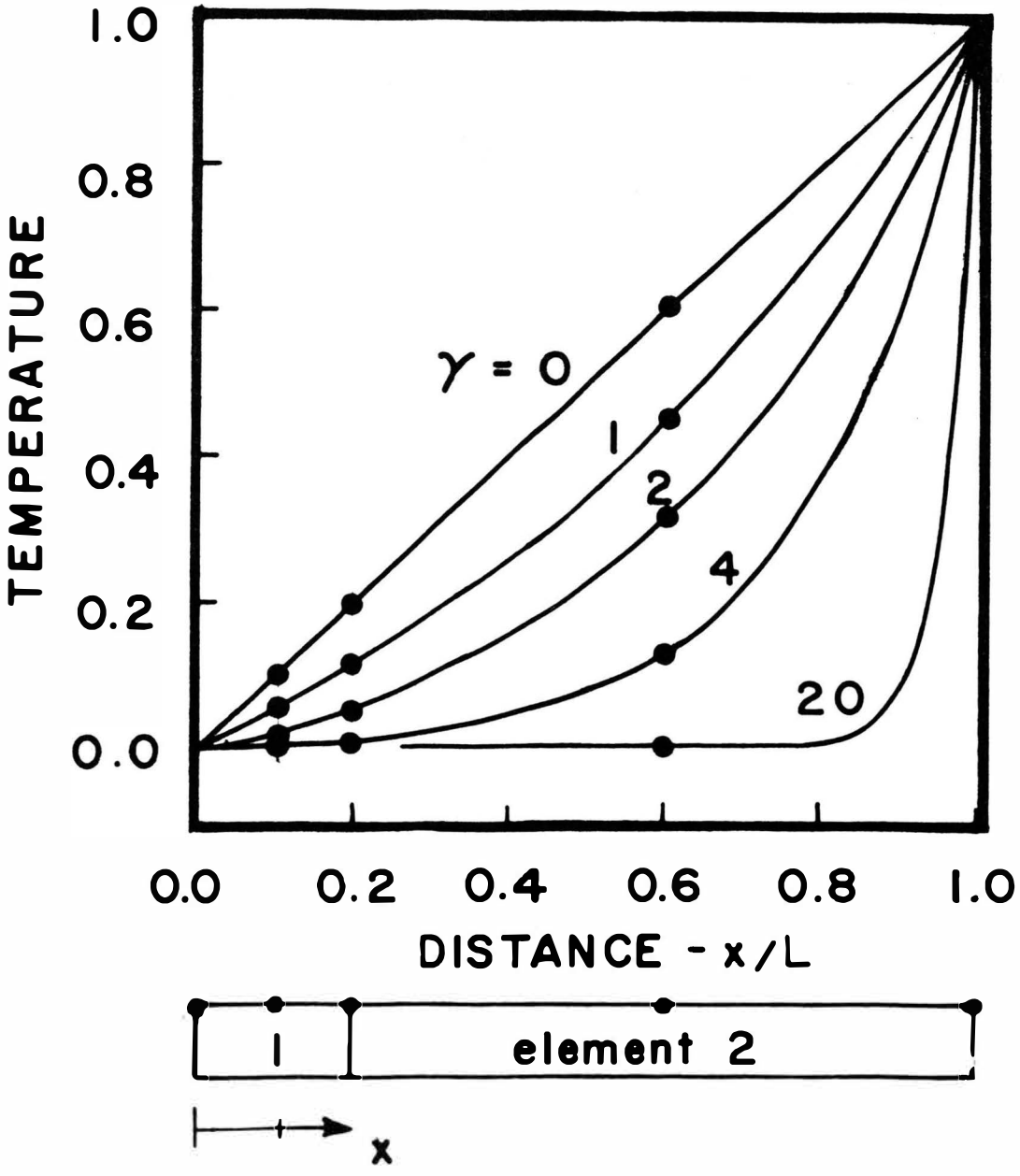
1.0
0.8
0.6
0.4
0.2
0.0
TEMPERATURE
γ = 0
1
2
4
20
0.0
0.2
0.4
0.6
0.8
1.0
DISTANCE - x/L
1
element 2
x

Figure 7

VITA

David Alan Dillard was born on September 3, 1954, in St. Mary's, Missouri. His primary and secondary eduction was received in Ste. Genevieve County, Missouri. He entered the University of Missouri-Rolla in 1972 and graduated with a Bachelor of Science in Engineering Mechanics in May 1976. After working at McDonnell Douglas Aircraft Company for a year, he returned to the University of Missouri-Rolla in August of 1977.